(4)

FURTHER RESEARCH

ON DYNAMICS OF MARINE ATMOSPHERES IN TROPICAL CYCLONES

by

Joseph Chi
Department of Mechanical Engineering
College of Physical Science, Engineering and Technology
University of the District of Columbia
Washington, DC 20008

Final Technical Report Submitted to:
Office of Naval Research
Project No. NR4226018-01
Grant No. N00014-84-K-0610/P00002

September 1989

SUMMARY

Under the Office of Naval Research(ONR) Grant No.N00014-84-K-0610, the University of the District of Columbia(UDC) has undertaken a basic research on dynamics of marine atmospheres in tropical cyclones with an objective of improving understanding of turbulence in cyclone vortices and efficiency of computer simulation for transfer of heat, moisture and momentum in marine planetary boundary layers of tropical cyclones. For this objective, UDC has performed the following four phases of effort:

I. Develop a mathematical model, using the second order turbulent closure equations, for simulating planetary boundary layers of tropical cyclones over the sea surface.

II. Calculate velocity, enthalpy and moisture distributions in planetary boundary layers of tropical cyclones over the sea surface.

III. Develop and instrument a laboratory vortex chamber for measuring the air/water interface turbulence and heat, moisture and momentum transfer.

IV. Develop a graphics-oriented interactive finite-element computer model to simulate transfer of heat, moisture and momentum in marine planetary boundary layers of tropical cyclones.

In this report, results of these four phases of effort are presented; and conclusions of this research program and recommendations for further research are described.

TABLE OF CONTENTS

LIST OF FIGURES

I. INTRODUCTION

The structure, evolution and motion of tropical cyclones are controlled by complex interaction of microscale, convective, mesoscale and synoptic processes. Convergence of moisture in the planetary boundary layer is a primary mechanism for organization of the convection in the inner core of an intense tropical cyclone. The convection, in turn, provides the diabatic heating necessary to sustain intensity of the tropical cyclone. Recent advances in turbulent modeling and computational techniques have made it possible to simulate simultaneous effects of numerous parameters on dynamics of tropical cyclones.

Under the Office of Naval Research(ONR) Grant No. N00014-84-K-0610, the University of the District of Columbia(UDC) has undertaken a basic research on dynamics of marine atmospheres in tropical cyclones with an objective of improving understanding of turbulence in cyclone vortices and efficiency of computer simulation for transfer of heat, moisture and momentum in marine planetary boundary layers of tropical cyclones. For this objective, UDC has performed the following four phases of effort:

I. Develop a mathematical model, using the second order turbulent closure equation, for simulating planetary boundary layers of tropical cyclones over the sea surface.

II. Calculate velocity, enthalpy and moisture distributions in planetary boundary layers of tropical cyclones over the sea surface.

III. Develop and instrument a laboratory vortex chamber for measuring the air/water interface turbulence and heat, moisture and momentum transfer.

IV. Develop a graphics-oriented interactive finite-element computer model to simulate transfer of heat, moisture and momentum in marine planetary boundary layers of tropical cyclones.

In this report, a mathematical model, using the second order turbulent closure equations, for simulating planetary boundary layers of tropical cyclones over the sea surface is described in Section 2. Results of calculated velocity, enthalpy and moisture distributions in planetary boundary layers of tropical cyclones over the sea surface are presented in Section 3. To increase confidence in the theory, calculated results are compared with laboratory test data in section 4. Development of a graphics-oriented interactive finite-element computer program for simulating the vortex flow constitutes a major effort in a latter part of this research program; and it will be detailed in Section 5 of this report. Conclusions of this research effort and recommendations for further research on dynamics of marine atmospheres in tropical cyclones are given in Section 6.

2. A MATHEMATICAL MODEL FOR SIMULATING VORTEX PLANETARY BOUNDARY LAYERS

Figure 1 shows schematically a vortex marine planetary boundary layer. The situation presents many interesting features which include the boundary layer heat, moisture and momentum transfer; turbulent energy production, dissipation and diffusion; strong influence of the gravitational, Coriolis and centrifugal forces; and influences of the air/sea interface roughness and liquid droplets entrainment. Under Phase I effort of this research program, a mathematical model, using the second order turbulent closure equations, for simulating planetary boundary layers of tropical cyclones over the sea surface has been developed.

Previous discussions of the turbulent transport theory (e.g., see Harlow and Hirt, 1969; Mellor and Yamada, 1974; and Leweller, 1981) yielded equations in rectangular coodinates for the turbulent stresses components and flux moments. For simulating the vortex marine planetary boundary layers, it is more convenient to use the cylindrical coodinates. Under Phase I effort of

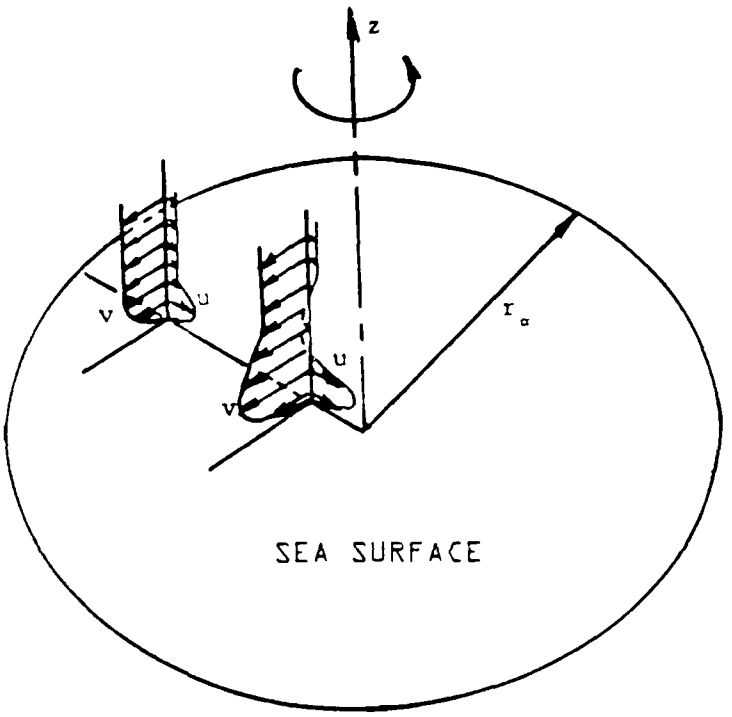

Figure 1 SKETCH OF VORTEX FLOW OVER A SEA SURFACE

this program, a second-order turbulent transport theory which uses the cylindrical coordinates and accounts for special features which are described in the preceding paragraph is derived. Details of derivation of the theory are described in Chi (1986); but a brief summary of the theory and its resultant equations are presented below in this section.

Starting from instantaneous conservation equations, mean equations of motion, and balances of energy and moisture for turbulent vortex flows were first derived. Transport equations for turbulent stress components, and enthalpy and moisture flux moments were then derived. Closure assumptions formulated by Chou (1945), Launder, Reese and Rodi (1975), and Lumley and Newman (1977) were finally used to complete the closure. In conclusion, a mathematical model for simulating vortex planetary boundary layers has been developed.

The coordinates are chosen so that z axis is vertical, and r axis is in the radial direction and ¢ is the azimuth angle. Equations governing mean motion and balances of mean enthalpy and moisture concentration can be written as:

$$\frac{\partial u}{\partial r} + \frac{u}{r} + \frac{\partial v}{r\partial \phi} + \frac{\partial w}{\partial z} = 0 \qquad (1)$$

$$\frac{\partial u}{\partial t} + u\frac{\partial u}{\partial r} + v\frac{\partial v}{r\partial \phi} + w\frac{\partial u}{\partial z} - \frac{v^2}{r} - fv$$

$$= -\frac{\partial p}{\rho \partial r} + \frac{\partial}{r\partial r}[2r\nu_t(\frac{\partial u}{\partial r})]$$

$$+ \frac{\partial}{r\partial \phi}[\nu_t(\frac{\partial u}{r\partial \phi} + \frac{\partial v}{\partial r} - \frac{v}{r})]$$

$$+ \frac{\partial}{\partial z}[\nu_t(\frac{\partial w}{\partial r} + \frac{\partial u}{\partial z})]$$

$$- \frac{2\nu_t}{r}(\frac{\partial v}{r\partial \phi} + \frac{u}{r}) \qquad (2)$$

$$\frac{\partial v}{\partial t} + u\frac{\partial v}{\partial r} + v\frac{\partial v}{r\partial \phi} + w\frac{\partial v}{\partial z} + \frac{uv}{r} + fu$$

$$= -\frac{\partial p}{\rho r\partial \phi} + \frac{\partial}{r\partial r}[r\nu_t(\frac{\partial u}{r\partial \phi} + \frac{\partial v}{\partial r} - \frac{v}{r})]$$

$$+ \frac{\partial}{r\partial \phi}[2\nu_t(\frac{\partial v}{r\partial \phi} + \frac{u}{r})]$$

$$+ \frac{\partial}{\partial z}[\nu_t(\frac{\partial w}{r\partial \phi} + \frac{\partial v}{\partial z})]$$

$$+ \frac{2\nu_t}{r}(\frac{\partial u}{r\partial \phi} + \frac{\partial v}{\partial r} - \frac{v}{r}) \qquad (3)$$

$$\frac{\partial w}{\partial t} + u\frac{\partial w}{\partial r} + v\frac{\partial w}{r\partial \phi} + w\frac{\partial w}{\partial z}$$

$$= -\frac{\partial p}{\rho \partial z} + \frac{\partial}{r\partial r}[r\nu_t(\frac{\partial w}{\partial r} + \frac{\partial u}{\partial z})]$$

$$+ \frac{\partial}{r\partial \phi}[\nu_t(\frac{\partial w}{r\partial \phi} + \frac{\partial v}{\partial z})]$$

$$+ \frac{\partial}{\partial z}(2\nu_t\frac{\partial w}{\partial z}) + \rho g s_v \qquad (4)$$

$$\frac{\partial h}{\partial t} + u\frac{\partial h}{\partial r} + v\frac{\partial h}{r\partial \phi} + w\frac{\partial h}{\partial z}$$

$$= \frac{\partial}{r\partial r}[\frac{r\nu_t}{\sigma_h}(\frac{\partial h}{\partial r})] + \frac{\partial}{r\partial \phi}[\frac{\nu_t}{\sigma_h}(\frac{\partial h}{r\partial \phi})]$$

$$+ \frac{\partial}{\partial z}[\frac{\nu_t}{\sigma_h}(\frac{\partial h}{\partial z})] \qquad (5)$$

$$\frac{\partial q}{\partial t} + u\frac{\partial q}{\partial r} + v\frac{\partial q}{r\partial \phi} + w\frac{\partial q}{\partial z}$$

$$= \frac{\partial}{r\partial r}[\frac{r\nu_t}{\sigma_q}(\frac{\partial q}{\partial r})] + \frac{\partial}{r\partial \phi}[\frac{\nu_t}{\sigma_q}(\frac{\partial q}{r\partial \phi})]$$

$$+ \frac{\partial}{\partial z}[\frac{\nu_t}{\sigma_q}(\frac{\partial q}{\partial z})] \qquad (6)$$

In these equations, u, v and w are the mean velocity components in the r, ¢ and z directions; t is the time, p the mean pressure, h the mean moist specific enthalpy which is defined as $(s+Lq_v)$, and q the mean total moisture mixing ratio which is defined as (q_v+q_ℓ). Here, s is the mean dry specific enthalpy which is defined as $C_p[T-(T_c-gz/C_p)]$, L the water latent heat of vaporization, C_p the constant pressure specific heat, T the temperature, T_c the standard temperature, q_v the water vapor mixing ratio, q_ℓ the liquid water mixing ratio, g the gravitational acceleration, f the Coriolis parameter, s_v the virtual dry specific enthalpy which is defined as $s(1+1.6090q_v-q)$, ρ_c the standard density, β the thermal expansion coefficient which is defined as $[1/(C_p T_c)]$, ν_t the turbulent kinematic viscosity, and σ_h the turbulent Prandtl number, and σ_h the turbulent Schmidt number.

In equations 1 through 6, the turbulent viscosity value ν_t can be calculated from the turbulent kinetic energy k and dissipation ε values as follows:

$$\nu_t = C_\nu \frac{k^2}{\varepsilon} \tag{7}$$

and values for k and ε in equation (7) can in turn be calculated by the equations:

$$\begin{aligned}
&\frac{\partial k}{\partial t} + u\frac{\partial k}{\partial r} + \frac{\partial k}{r\partial \phi} + w\frac{\partial k}{\partial z} \\
&\quad = \nu_t\{2[(\frac{\partial u}{\partial r})^2 + (\frac{\partial v}{r\partial \phi} + \frac{u}{r})^2 + (\frac{\partial w}{\partial z})^2] + (\frac{\partial u}{r\partial \phi} + \frac{\partial v}{\partial r} + \frac{v}{r})^2 \\
&\qquad + (\frac{\partial w}{\partial r} + \frac{\partial u}{\partial z})^2 + (\frac{\partial w}{r\partial \phi} + \frac{\partial v}{\partial z})^2] - \frac{\beta g}{\sigma_s}\frac{\partial s_v}{\partial z}\} \\
&\qquad + \frac{\partial}{r\partial r}(\frac{r\nu_t}{\sigma_k}\frac{\partial k}{\partial r}) + \frac{\partial}{r\partial \phi}(\frac{\nu_t}{\sigma_k}\frac{\partial k}{r\partial \phi}) + \frac{\partial}{\partial z}(\frac{\nu_t}{\sigma_k}\frac{\partial k}{\partial z}) \\
&\qquad - \varepsilon
\end{aligned} \tag{8}$$

$$\frac{\partial \varepsilon}{\partial t} + u\frac{\partial \varepsilon}{\partial r} + v\frac{\partial \varepsilon}{r\partial \phi} + w\frac{\partial \varepsilon}{\partial z}$$

$$= 1.45\frac{\varepsilon}{k}\nu_t\{2[(\frac{\partial u}{\partial r})^2 + (\frac{\partial v}{r\partial \phi} + \frac{u}{r})^2 + (\frac{\partial w}{\partial z})^2] + (\frac{\partial u}{r\partial \phi} + \frac{\partial v}{\partial r} + \frac{v}{r})^2$$

$$+ (\frac{\partial w}{\partial r} + \frac{\partial u}{\partial z})^2 + (\frac{\partial w}{r\partial \phi} + \frac{\partial v}{\partial z})^2 - \frac{\beta g}{\sigma_s}\frac{\partial s_v}{\partial z}\}$$

$$+ \frac{\partial}{r\partial r}(\frac{r\nu_t}{\sigma_\varepsilon}\frac{\partial \varepsilon}{\partial r}) + \frac{\partial}{r\partial \phi}(\frac{\nu_t}{\sigma_\varepsilon}\frac{\partial \varepsilon}{r\partial \phi}) + \frac{\partial}{\partial z}(\frac{\nu_t}{\sigma_\varepsilon}\frac{\partial \varepsilon}{\partial z})$$

$$- 2\frac{\varepsilon^2}{k} \qquad (9)$$

In quations (8) and (9), the virtual dry specific enthalpy value s_v value is related to the mean moist specific enthalpy h and mean total moisture mixing ratio q values by the equations:

$$\frac{\partial s_v}{\partial z} = \nu_t c_s[\frac{\partial h}{c_h \partial z} + (0.609\xi - 1)\frac{L\partial q}{c_q \partial z}] \qquad (10)$$

$$\frac{\partial s_v}{\partial z} = \nu_t c_s[\frac{(1 + 1.609\gamma\xi)\partial h}{(1 + \gamma)c_h \partial z} - \frac{\xi L \partial q}{c_q \partial z}] \qquad (11)$$

where γ and ξ are equal to $(L/C_p)(\partial q/\partial T)$ and $(C_p T/L)$, respectively.

Equations (1) through (11) with appropriate initial and boundary conditions now constitute a complete equation set which may be solved to simulate marine planetary boundary layers of tropical cyclones.

3. HEAT, MOISTURE AND MOMENTUM DISTRIBUTIONS IN VORTEX BOUNDARY LAYERS

The turbulent models discussed in Section 2 above can be used to simulate the marine planetary boundary layer of tropical cyclones. As an example, a

simple case which will first be considered is that the flow is quasi-steady and axisymmetrical and that the boundary layer thickness is much less than the vortex radial length (i.e., for a region of the vortex boundary layer far away from the vortex center). Governing equations for this problem can be derived from equations which are discussed in Section 2 above and they may be written as:

$$\frac{\partial ur}{r\partial r} + \frac{\partial w}{\partial z} = 0 \tag{12}$$

$$u\frac{\partial u}{\partial r} + w\frac{\partial u}{\partial z} = [(f + \frac{v}{r}) - (f + \frac{v_\infty}{r})v_\infty] + \frac{\partial}{\partial z}(\nu_t\frac{\partial u}{\partial z}) \tag{13}$$

$$u\frac{\partial v}{\partial r} + w\frac{\partial v}{\partial z} = \frac{\partial}{\partial z}(\nu_t\frac{\partial v}{\partial z}) \tag{14}$$

$$u\frac{\partial h}{\partial r} + w\frac{\partial h}{\partial z} = \frac{\partial}{\partial z}(\frac{\nu_t}{c_h}\frac{\partial h}{\partial z}) \tag{15}$$

$$u\frac{\partial q}{\partial r} + w\frac{\partial q}{\partial z} = \frac{\partial}{\partial z}(\frac{\nu_t}{c_q}\frac{\partial q}{\partial z}) \tag{16}$$

$$u\frac{\partial k}{\partial r} + w\frac{\partial k}{\partial z} = \frac{\partial}{\partial z}(\frac{\nu_t}{c_k}\frac{\partial k}{\partial z}) + \nu_t[(\frac{\partial u}{\partial z})^2 + (\frac{\partial v}{\partial z})^2 - \frac{\beta g}{c_s}\frac{\partial s_v}{\partial z}] - \varepsilon \tag{17}$$

$$u\frac{\partial \varepsilon}{\partial r} + w\frac{\partial \varepsilon}{\partial z} = \frac{\partial}{\partial z}(\frac{\nu_t}{c_\varepsilon}\frac{\partial \varepsilon}{\partial z}) + 1.45\frac{\varepsilon}{k}\nu_t[(\frac{\partial u}{\partial z})^2 + (\frac{\partial v}{\partial z})^2 - \frac{\beta g}{c_s}\frac{\partial s_v}{\partial z}] - C_\varepsilon\frac{\varepsilon^2}{k} \tag{18}$$

where

$$\nu_t = C_\nu \frac{k^2}{\varepsilon} \tag{19}$$

$$\frac{\partial s_v}{\partial z} = \nu_t \sigma_s \left[\frac{\partial h}{c_h \partial z} + \frac{(0.609\xi - 1)L}{\sigma_q} \frac{\partial q}{\partial z}\right] \quad \text{(For Clear Region)} \tag{20}$$

$$\frac{\partial s_v}{\partial z} = \nu_t \sigma_s \left[\frac{(1 + 1.609\xi\gamma)}{(1 + \gamma)c_h} \frac{\partial h}{\partial z} + \frac{\xi L}{\sigma_q} \frac{\partial q}{\partial z}\right] \quad \text{(For Cloudy Region)} \tag{21}$$

$$C_\nu = 0.09\exp[-2.5/(1+0.02Re_t)] \tag{22}$$

$$C_\varepsilon = 2[1 - 0.3\exp(-Re_t^2)] \tag{23}$$

$$Re_t = \frac{k^2}{\varepsilon} \tag{24}$$

$$(c_h, \sigma_q, \sigma_s, \sigma_k, \sigma_\varepsilon) = (0.9, 0.9, 0.9, 1.0, 1.3) \tag{25}$$

A finite difference numerical procedure has been developed and a computer program has been written for solving the above set of equations with appropriate vortex boundary conditions to simulate the transfer of heat, moisture and momentum in turbulent vortex flows over the water surface. Details of this development has been published by Chi (1987), and a reprint of the paper is appended to this report (see Appendix A).

As an example, the computer results for a hypothetic tropical cyclone under conditions shown in table 1 are presented and discussed below:

TABLE 1

Maximum tangential Wind v+ at 1 km Altitude	52 m/s

Radius at Which Max. v+ Occurs	40 km
Temperature at 1 km Altitude	273 K
Coriolis Force Coefficient	1×10^{-5} s^{-1}
Temperature at Sea Surface	288 K

Figure 2 shows distributions of radial and tangential components (u_+ and v_+) of the cyclone mean velocity at the 1-km altitude. Radial and tangential components (u and v) of the boundary-layer velocity are plotted versus height z at several radii r in figure 3 and 4, respectively. Values for the vertical-velocity component w_+ at the 1-km altitude are plotted in figure 5. The boundary-layer specific enthaly ($h-h_+$) and moisture ratio ($q-q_+$) values are plotted versus height z at several radii in figures 6 and 7, respectively. Figure 8 show a distribution of the boundary-layer turbulent kinetic energy.

Several interesting marine vortex boundary layer characteristics can be observed from these figures. For the region far above the ground (i.e., at high altidude), it can be seen in figure 4 that tangential velocity dominates. The balance of force for this region is, therefore, a balance of pressure gradient and combination of the centrifugal and Coriolis forces. Near the sea surface, retardation of the tangential velocity can be seen in figure 4. This retardation is accompanied by a reduction in centrifugal and Coriolis forces. The balance of pressure, centrifugal and Coriolis forces is thereby destroyed. The flow in this region is then characterized by entrainment of the flow into the boundary layer as indicated by the large induced radial velocity shown in figure 3 and the induced downward flow (i.e., negative w_+ values) shown in figure 5. Figures 6 and 7 show large enthalpy and moisture values at vicinity of the sea surface and their decreased values at large altitude. Advection diffusion of the turbulent energy in the boundary layer can be observed from distribution of k values shown in figure 8.

Detailed measurement of the boundary-layer values in tropical cyclone is

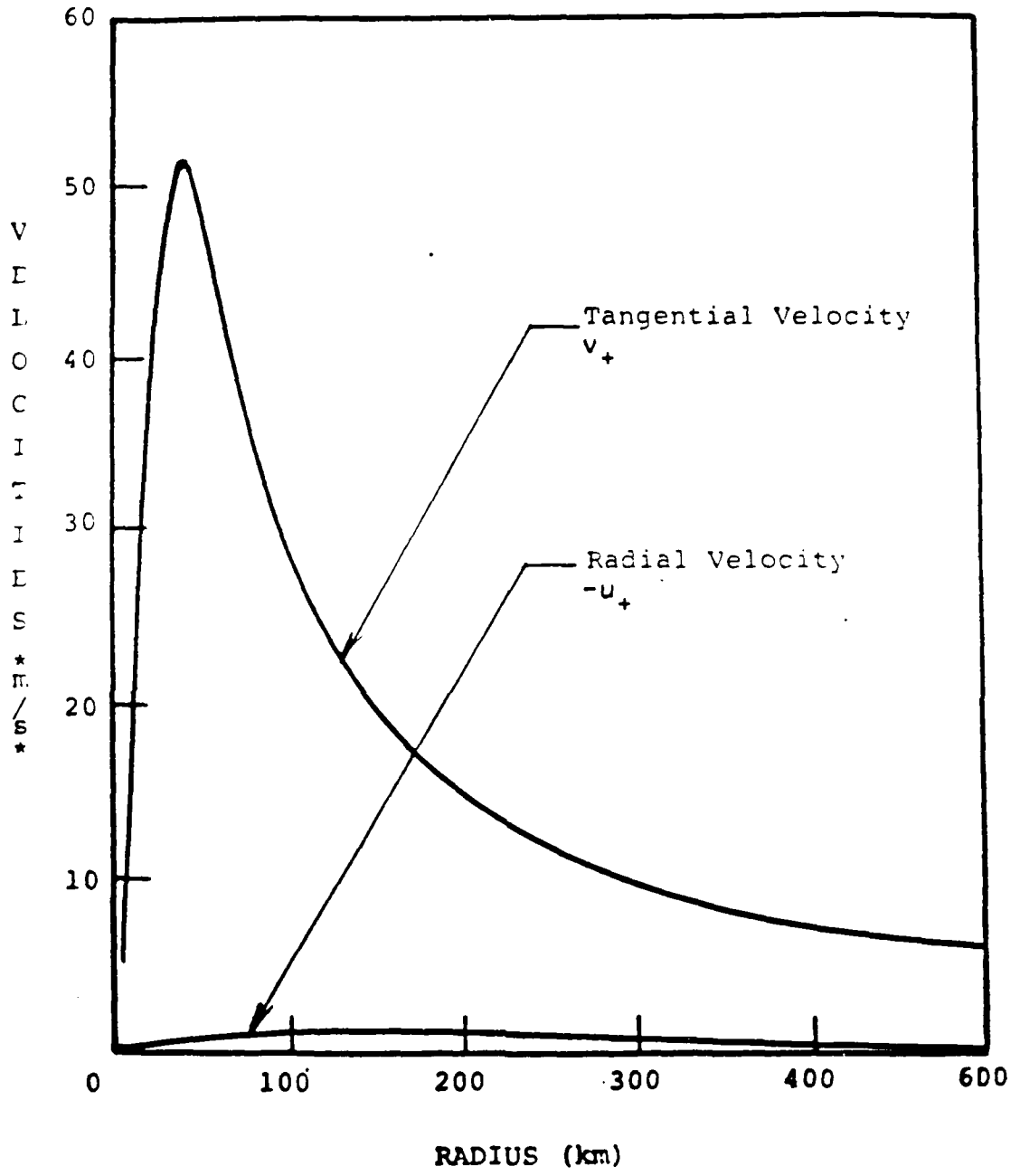

FIGURE 2 RADIAL AND TANGENTIAL VELOCITY DISTRIBUTIONS ($-u_+$ & v_+) OF A TROPICAL CYCLONE AT 1-KM ALTITUDE

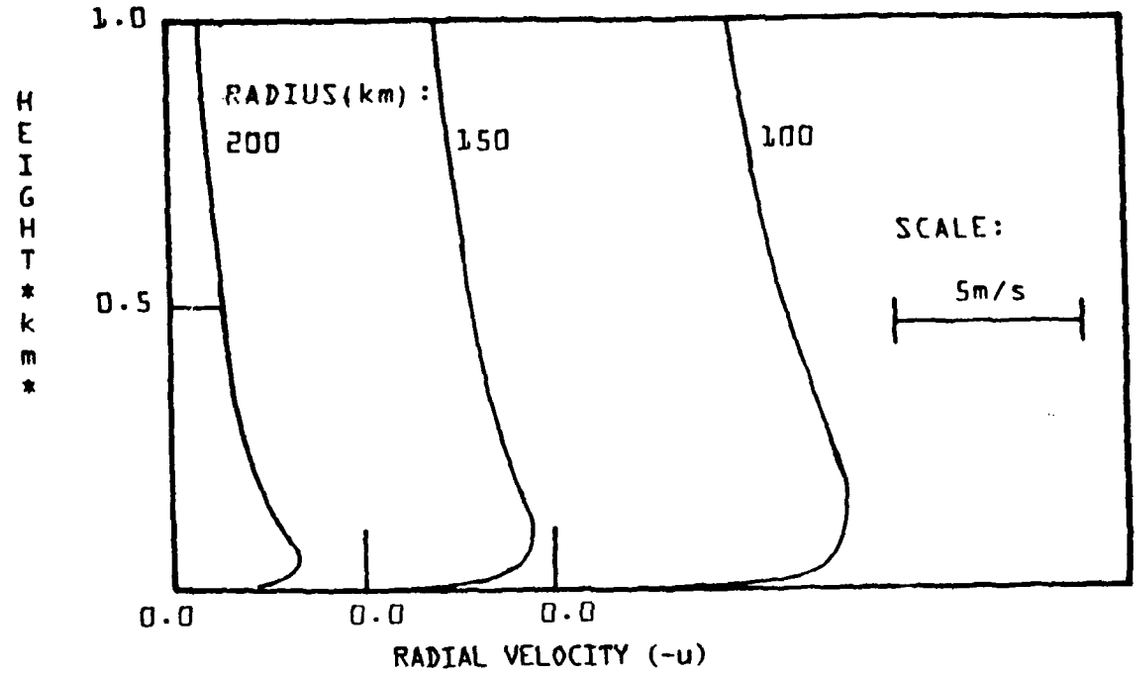

FIGURE 3 COMPUTER SIMULATED RADIAL VELOCITY DISTRIBUTION (-u) IN THE BOUNDARY LAYER OF A TROPICAL CYCLONE

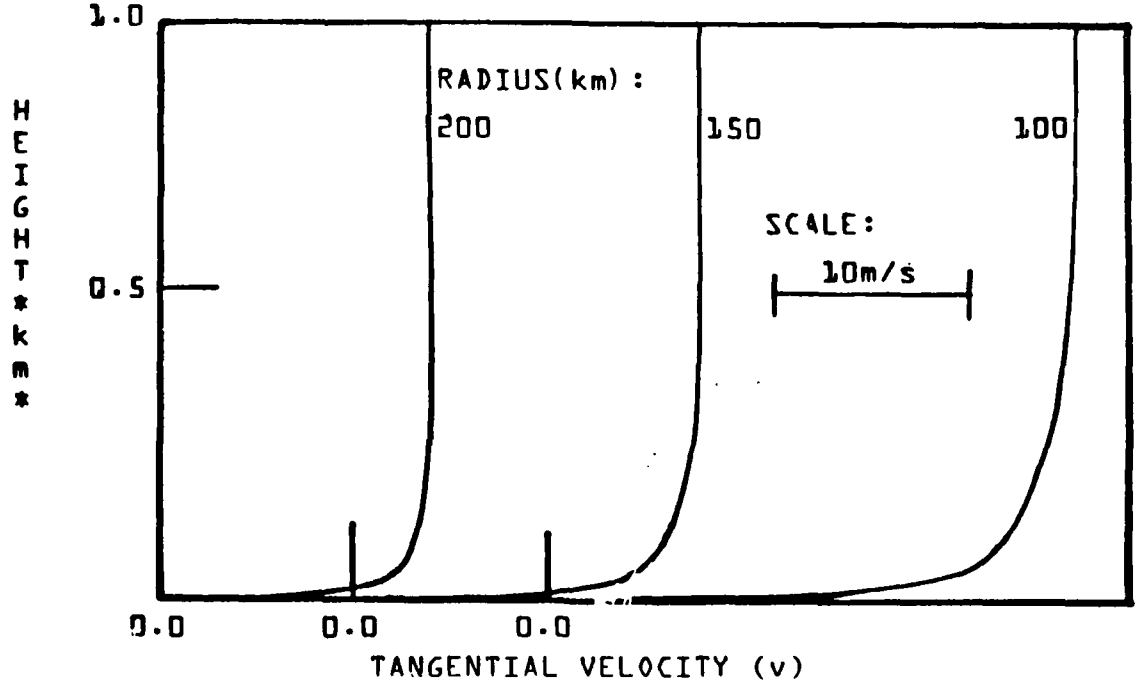

FIGURE 4 COMPUTER SIMULATED TANGENTIAL VELOCITY DISTRIBUTION (v) IN THE BOUNDARY LAYER OF A TROPICAL CYCLONE

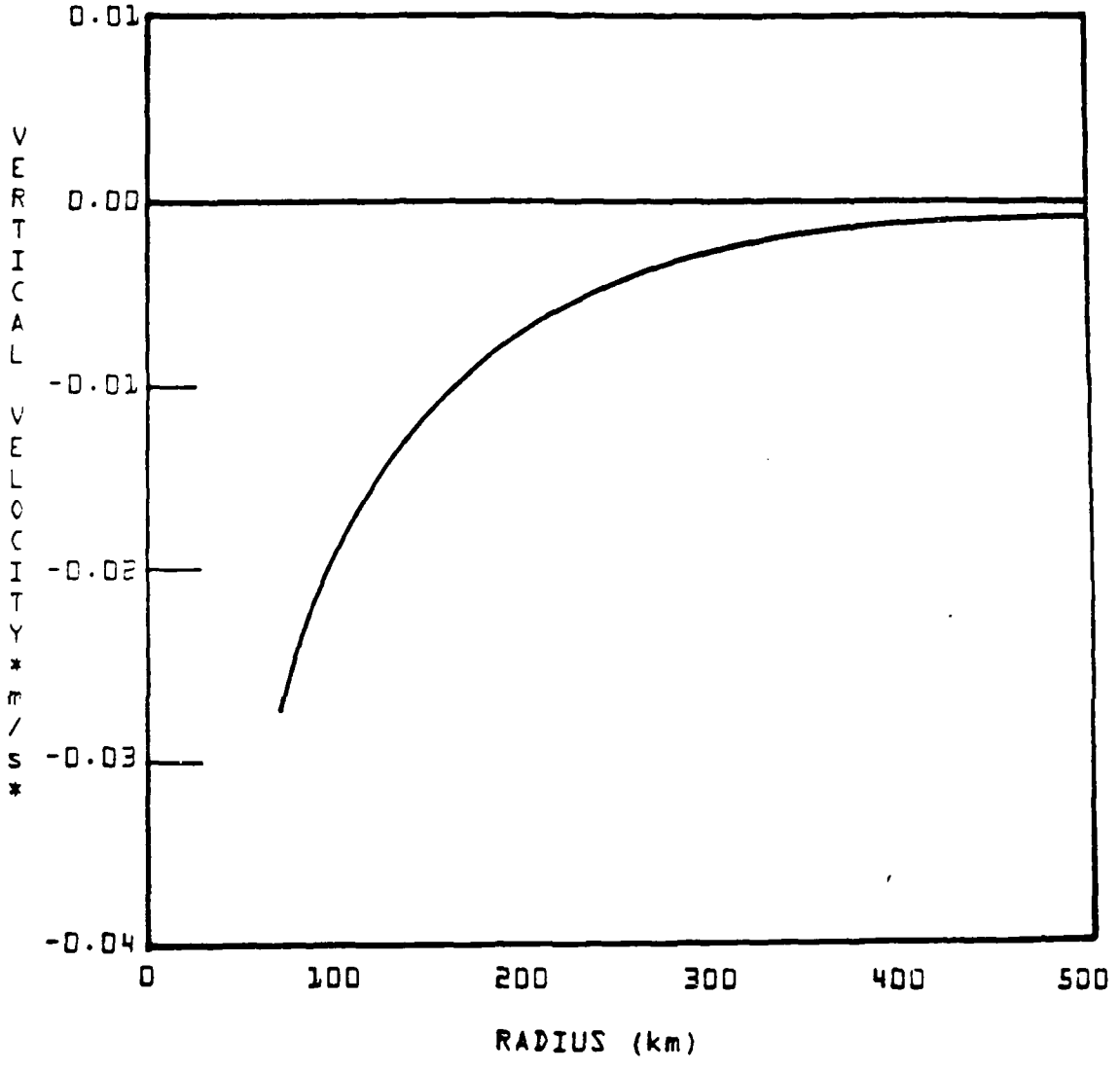

FIGURE 5 COMPUTER SIMULATED VERTICAL VELOCITY DISTRIBUTION (w_+) OF A TROPICAL CYCLONE AT 1-KM ALTITUDE

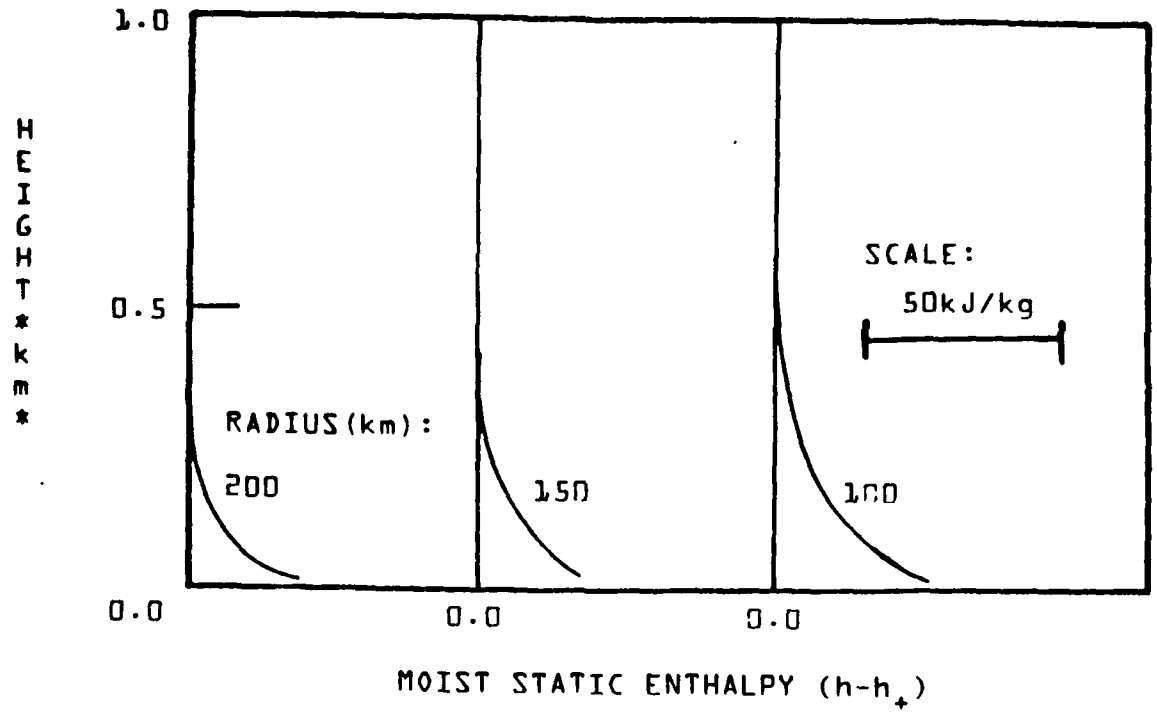

FIGURE 6 COMPUTER SIMULATED MOIST STATIC ENTHALPY DISTRIBUTION ($h-h_+$) IN THE BOUNDARY LAYER OF A TROPICAL CYCLONE

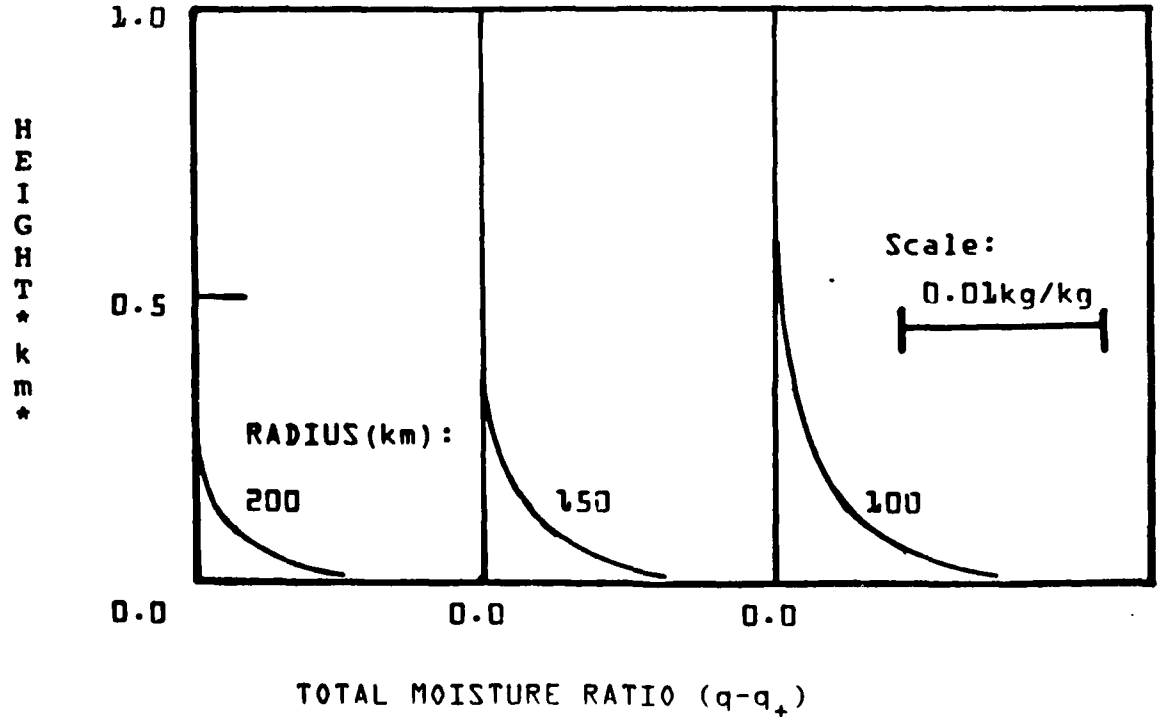

FIGURE 7 COMPUTER SIMULATED TOTAL MOISTURE RATIO DISTRIBUTION ($q-q_+$) IN THE BOUNDARY LAYER OF A TROPICAL CYCLONE

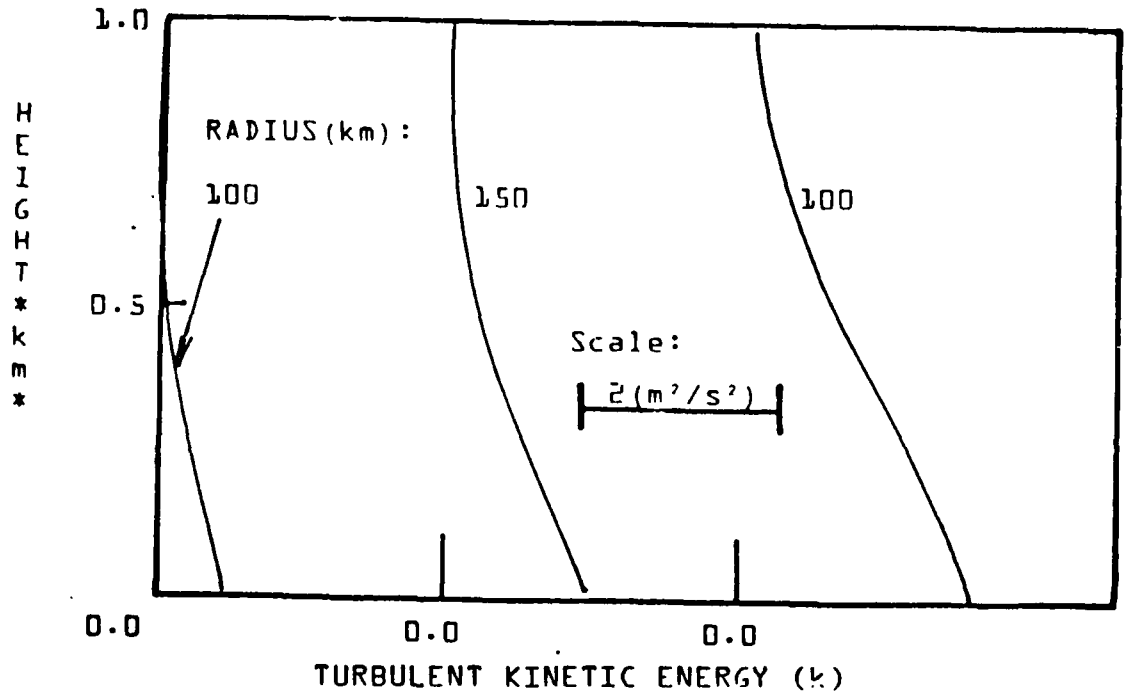

FIGURE 8 COMPUTER SIMULATED TURBULENT KINETIC ENERGY DISTRIBUTION (k) IN THE BOUNDARY LAYER OF A TROPICAL CYCLONE

difficulty if not impossible. A laboratory vortex chamber with air/water interface has been built at UDC. Some UDC test data are presented and discussed in the next section of the report.

4. COMPARISON OF CALCULATED RESULTS WITH LABORATORY TEST DATA

In order to establish confidence in the computer simulated results, measurements of the turbulent vortex flow have been made on a UDC vortex chamber. Figure 9 shows a schematic diagram of the UDC vortex chamber. The chamber overall dimension is 55-cm diameter by 90-cm high. It generates an air vortex of 30.48-cm diameter by 14-cm high. The vortex is generated by forcing air through 24 evenly spaced vanes of 15-cm high placed on a 30.48-cm diameter pitch circle. The swirling air discharges from the chamber through a 3.81-cm diameter hole located at center of the chamber's top disk. Bottom of the swirling air is in contact with a pool of water which can be maintained at a constant depth and at desired temperatures. The chamber is instrumented with both the TSI hot-film anemometer and laser doppler velocimeter. An IBM PC has been used for online data acquisition and processing.

Figure 10 shows an example of the measured radial u_+ and tantengial v_+ components of air velocity in the main vortex flow outside the boundary layer. Also can be seen in this figure is that u_+ and v_+ values for this vortex flow can be correlated accurately by the equations:

$$u+ = \frac{(u+)_\infty r_\infty}{r}\{1 - \exp[-\frac{2.506\nu_t}{(u+)_\infty r_\infty}(\frac{r}{r_m})^2]\} \qquad (26)$$

$$v+ = \frac{1.4v_m r_m}{r}\{1 - \exp[-1.253(\frac{r}{r_m})^2]\} \qquad (27)$$

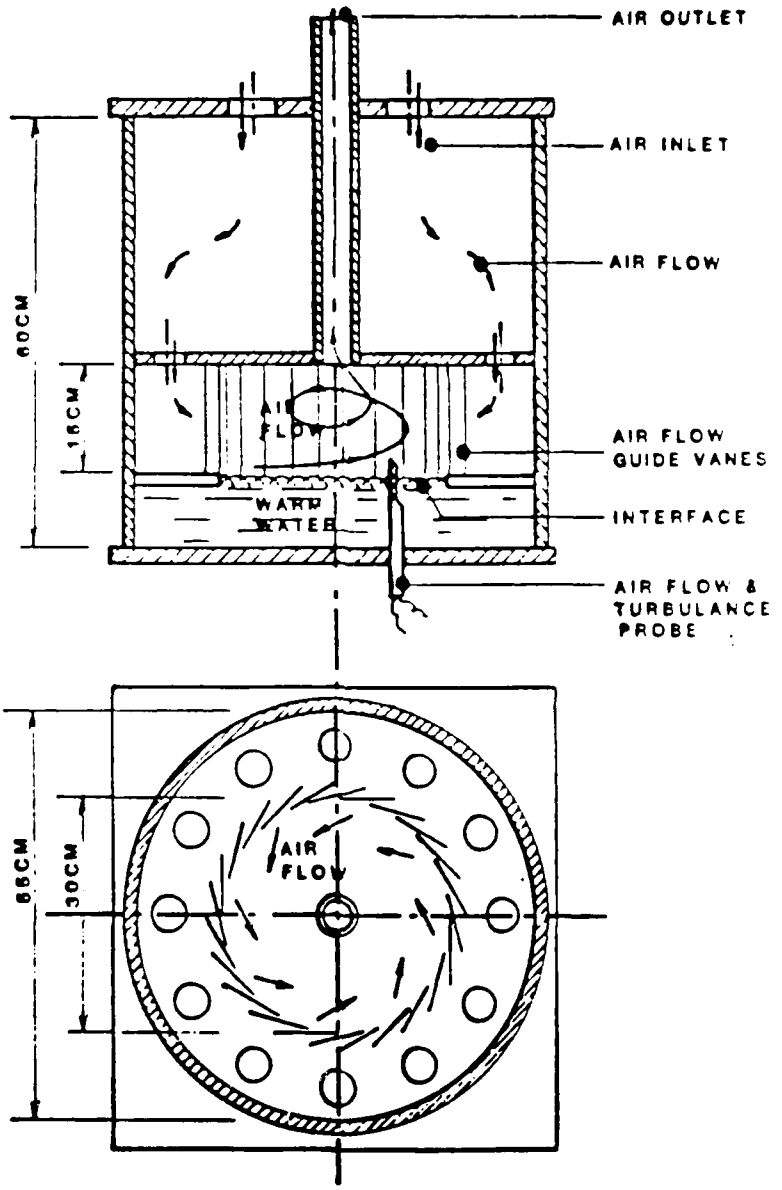

FIGURE 9 SCHEMATIC OF A UDC LABORATORY VORTEX TEST CHAMBER

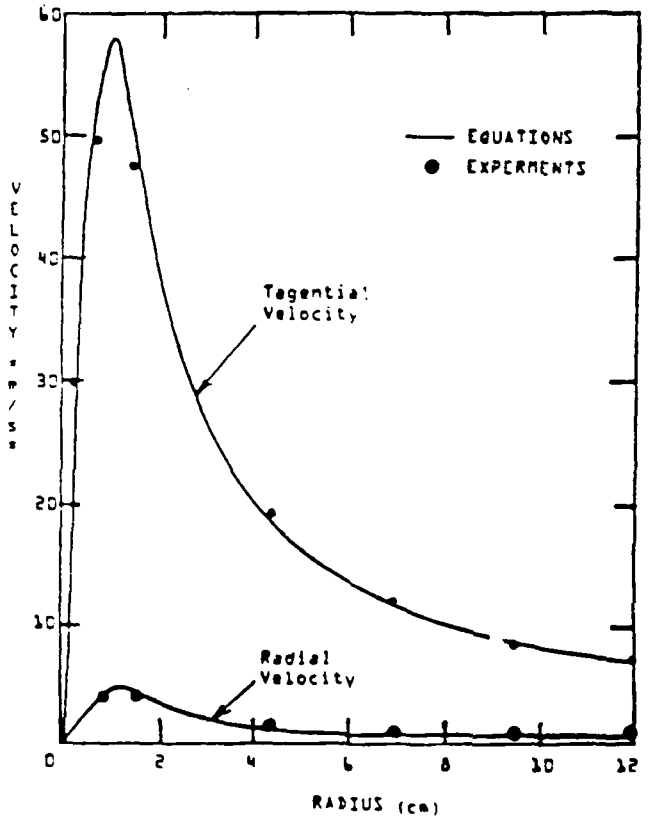

FIGURE 10 MAIN VORTEX u_+ and v_+ UNDER A TEST CONDITION

where suffix + represents values at vortex main flow, suffix ∞ represents values at large radius, and suffix m represents values at a position in the main flow where the vortex tangential velocity is maximum.

Measurements in the boundary layer have so far been made only with the hot-film probe for the air flow over solid end walls. Results of the measured radial u and tangential v values inside the vortex boundary layers on the smooth and rough end walls are shown in figures 11 and 12, respectively. For comparison, computer simulated results under same conditions as experiments are also plotted in these figures. Excellent agreement between theory and experiments can be seen in these figures.

5. A GRAPHICS-ORIENTED INTERACTIVE SIMULATION MODEL FOR TRANSFER OF HEAT, MOISTURE AND MOMENTUM

The last phase of effort under this program was spent in developing a graphics interactive turbulent simulation computer program based upon the Galerkin's finite element method. A peculiar feature of the finite-element method is the division of domain into a finite number of elements. A set of basis functions is locally defined over each element so that one only needs to consider the governing equations for individual elements. After the element equations are obtained, a simple assembly of these equations over all the elements yields the global system of equations. Since the shape and size of individual elements are very flexible, local refinement of resolution can be easily obtained for regions of strong gradients. Irregularly shaped domains can also be easily divided into elements without coding difficulties. These flexibilities of the finite-element method make it especially useful for modeling heat, moisture and momentum transport in the marine boundary layers for which mesh nesting and complex interactions are important. In addition, ability of discretization allows easy interfacing of the finite element computer program with the interactive graphics software. The author and his

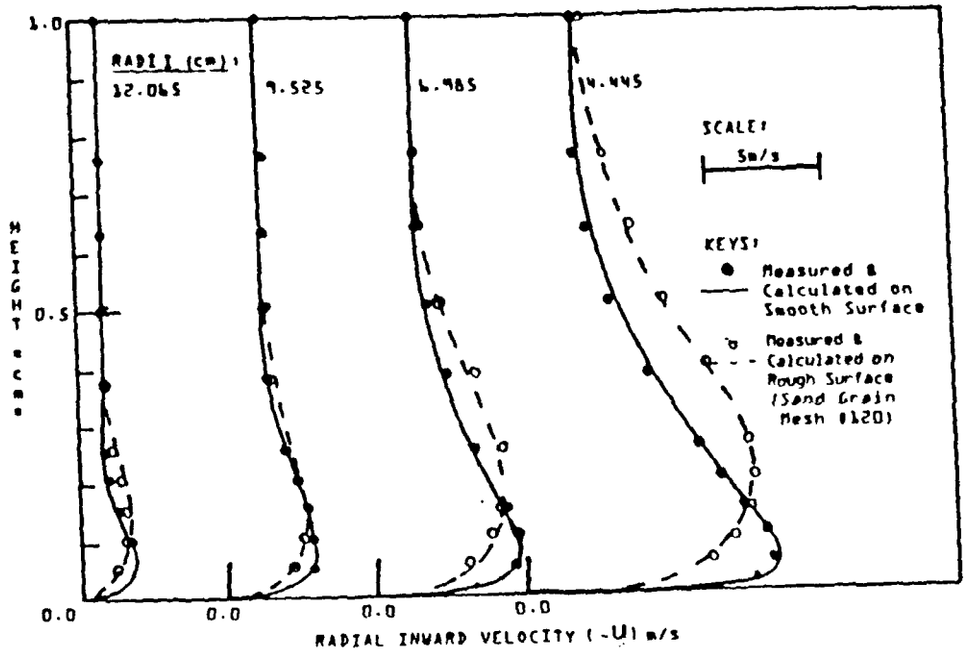

FIGURE 11 COMPARISON OF TEST DATA WITH COMPUTER SIMULATED RADIAL VELOCITY (-u) VALUES

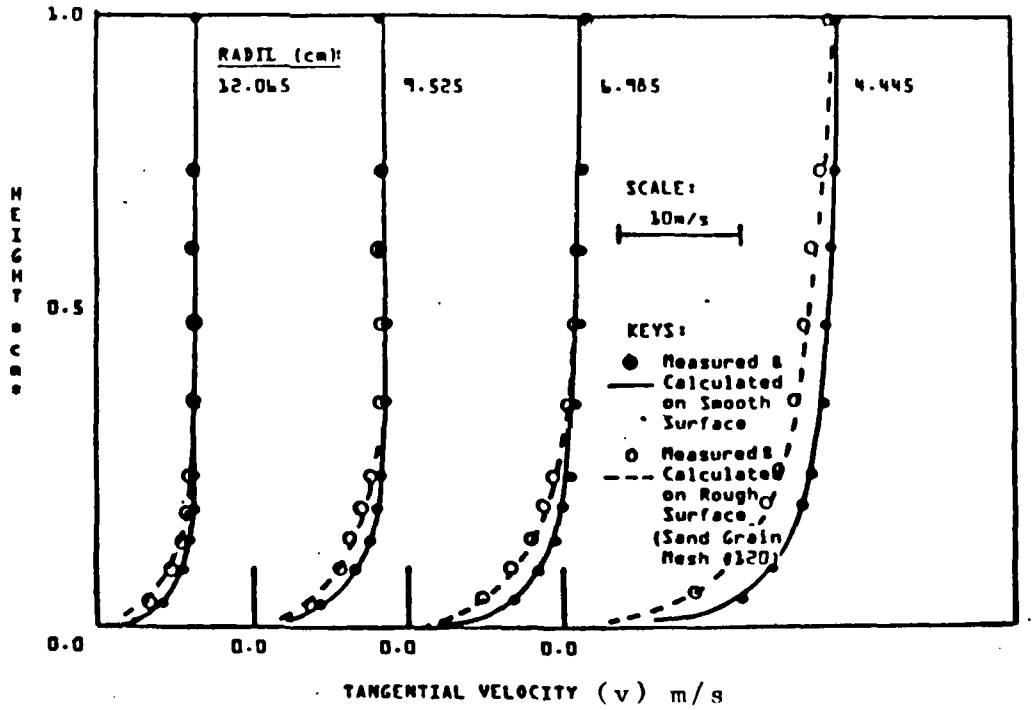

FIGURE 12 COMPARISION OF TEST DATA WITH COMPUTER SIMULATED BOUNDARY TANGENTIAL VELOCITY (v) VALUES

co-workers have been developing under this Grant a finite element analysis computer program for simulating three dimensional tranportation of momentum, moisture and enthalpy, and have so far obtained solutions for the one- and two-dimensional problems. In addition, the UDC's finite-element computer programs have been interfaced with the PDA's PATRAN graphics-oriented software package. This interface has allowed PATRAN to be used for model creation and results presentation under an interactive graphics-oriented environment and the UDC's finite element computer program to be used for analysis.

For convenience of documentation, development todate of the graphics-oriented interactive finite element computer program at UDC is presented below in several sub-sections as follows:

- Equations Under Consideration
- Finite Element Formulation
- Solution Procedures and Computer Programming
- Interfacing of the UDC Finite-Element Programs with the Graphics-Oriented PATRAN Modeling Pre- and Post-Processor
- Results and Discussion.

5.1 Equations Under Consideration

The equations under consideration are conservation equations derived in Section 2 of the report. Limiting discussions in this section to problems of momentum transfer in two dimensions and assuming constant turbulent viscosity, the following governing equations in nondimensional tensor form may be obtained:

$$M(U_i) = \frac{\partial U_i}{\partial \tau} + \frac{\partial}{\partial X_j}(U_i U_j + \frac{1}{\rho_0} P\delta_{ij} - \frac{1}{Re}\frac{\partial U_i}{\partial X_j} - FU_2\delta_{1i} + FU_1\delta_{2i})$$

$$= 0 \qquad (28)$$

$$C(\rho_o) = \frac{\partial U_j}{\partial X_j} \tag{29}$$

$$B(U_i) = a_i U_i + \frac{1}{Re} \frac{\partial U_i}{\partial X_j} \bar{n}_j + b_i \tag{30}$$

where suffices i and j follow the usual tensor rules, and their values are either one or two for reference to nondimensional quantities in the x or y direction. The nondimensional quantities in these equations in terms of reference length and velocity v are defined as follows:

Nondimensional Corrilis Component, $F = \frac{f\ell_r}{v_r}$ (31)

Nondimensional Pressure, $P = \frac{p}{\rho_o v_r^2}$ (32)

Nondimensional Reynolds Number, $Re = \frac{v_r \ell_r}{\nu_t}$ (33)

Nondimensional Velocity in x-Direction, $U = U_1 = \frac{u}{v_r}$ (34)

Nondimensional Velocity in y-Direction, $V = U_2 = \frac{v}{v_r}$ (35)

Nondimensional Distance in x-Director, $X = X_1 = \frac{x}{\ell_r}$ (36)

Nondimensional Distance in y-Direction, $Y = X_2 = \frac{y}{\ell_r}$ (37)

Nondimensional Time, $\tau = \frac{tv_r}{\ell_r}$ (38)

5.2 Finite Element Formulation

Construction of a Galerkin finite element algorithm is now to be made to solve for the velocity components U1(=U) and U2(=V) from equation (28). The flow domain to be analyzed is divided into small subdomains call finite elements. Governing equations are then transformed into finite element equations. Finally, the finite element equations are assembled into a global system of equations which can be solved to yield simulation results for the problem.

In the present analysis, rectangular finite elements are used to discretizing the flow domain. The rectangular elements have four nodes. The interpolating equations for velocity in an element shown in figure 13 can be written as:

$$U_i(\eta_1,\eta_2) = N(\eta_1,\eta_2)\{UI(\tau)\} \tag{39}$$

where

$$N(\eta_1,\eta_2) = \tfrac{1}{4}\begin{Bmatrix} (1-\eta_1)(1-\eta_2) \\ (1+\eta_1)(1-\eta_2) \\ (1+\eta_1)(1+\eta_2) \\ (1-\eta_1)(1+\eta_2) \end{Bmatrix}^T \tag{40}$$

and $\eta_1 = X1/a = X/a$ and $\eta_2 = X2/b = Y/b$.

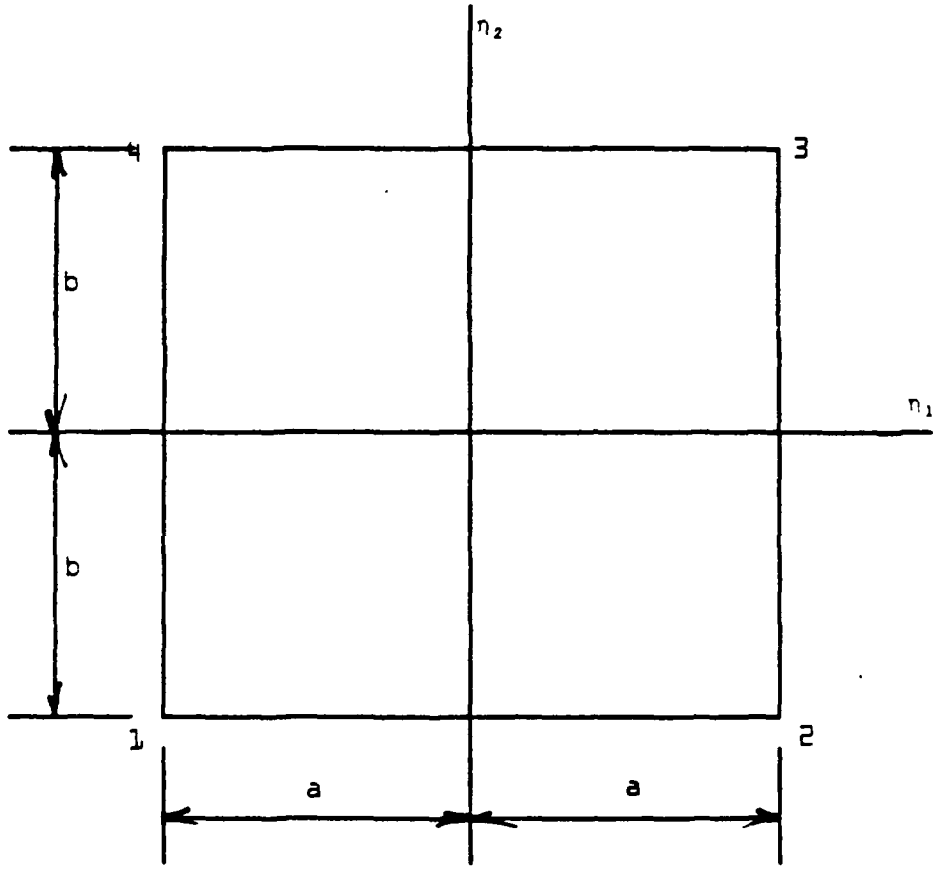

FIGURE 13 SKETCH OF A RECTANGULAR FINITE-ELEMENT DOMAIN

Equation (39) expresses U and V values in terms of natural coordinates and nodal values UI which is equal to U1 or U2. Construction of finite element solution algorithm for equation (28) subjects to several constraints. It is firstly required to satisfy the boundary condition equation (30), secondly to equate gradient of the convection part of equation (28) to zero for controlling nonlinearly induced instability and dispersion error,i.e.,

$$\frac{\partial}{\partial X_j} M(U_i) = \frac{\partial}{\partial X_j}\left(\frac{\partial U_i}{\partial \tau} + U_j \frac{\partial U_i}{\partial X_j}\right) = 0 \tag{41}$$

and finally to satify the panalty function which equates pressure to the continuiy function define by equation (29), i.e.:

$$\Pi(P) = P + \lambda \frac{\partial U_j}{\partial X_j} \tag{42}$$

Application of the Galerkin weighted residue method to governing equation (28) for individual finite elements with constraints of equations (30), (41) and (42), and substitution of discretization equation (39) can now be made to yield the element algorithm statement:

$$\int_{\Omega_e} \{N\} M(U_i) d\Omega - \beta_j \int_{\Omega_e} \{N\} \frac{\partial}{\partial X_j} M(U_i) d\Omega + \int_{\Gamma_e} \{N\} B(U_i) d\Gamma + \int_{\Omega_e} \frac{\partial}{\partial X_i} \{N\} \Pi(P) d\Omega = 0 \tag{43}$$

The resultant element contributions can be assembled into a global system of ordinary differential equations with respect to the nondimensional time τ as follows:

$$[CI]\{UI\}' + [KI]\{UI\} + [KIJ]\{UJ\} + \{SI\} = 0 \tag{44}$$

Here, [CI] is the capacity matrix, [KI] represents the convection operator in equation (28), [KIJ] provides the complete cross-coupling between the nodel {UI} and {UJ} values, and {SI} is any source term.

5.3 Solution Procedure and Computer Program UDCFLOW

An implicit finite-difference integration procedure is used to evaluate numerically the ordinary differential equation set (44). With θ, which is within zero and one, as an implicit parameter, the differential equation set (44) can be approximated by the algebraic equation set:

$$\begin{aligned} FI &= [CI]\, UI^{P}_{n+1} - UI_n \\ &\quad + \theta(\Delta\tau)([KI]^{P}_{n+1}\{UI\}^{P}_{n+1} + [KIJ]^{P}_{n+1}\{UJ\}^{P}_{n+1} + \{SI\}^{P}_{n+1}) \\ &\quad + (1-\theta)(\Delta\tau)([KI]_n\{UI\}_n + [KIJ]_n\{UJ\}_n + \{SI\}_n) \end{aligned} \tag{45}$$

Starting from guessed UI values, corrections for UI values can be calculated using the Newton iteration algorithm:

$$[J(FI)]^{P}_{n+1}\ \{\delta UI\}^{P+1}_{n+1} = -\{FI\}^{P}_{n+1} \tag{46}$$

Iterated solutions can then be defined as:

$$\{UI\}^{P+1}_{n+1} = \{UI\}^{P}_{n+1} + \{\delta UI\}^{P+1}_{n+1} \tag{47}$$

Here the Newton algorithm Jacobian is constructed as:

$$[J(FI)] = \frac{\partial\{FI\}}{\partial\{UJ\}} \tag{48}$$

The process is repeated until a preset convergence criterion is met.

A computer program UDCFLOW has been written using the above-described finite-element algorithm and calculation procedure for evaluating distributions of U and V in X and Y domain Ω at different time τ. To facilitate the use of the program, the UDCFLOW has been interfaced with the PDA's PATRAN graphics-oriented modeling pre- and post-processors.

5.4 UDCFLOW and PATRAN Interface

UDCFLOW is a finite element computer program for simulating transient flow of fluid in two dimensional fields. To facilitate efficient flow simulation, the UDCFLOW has been intergrated with the PATRAN software package for graphic pre- and post-processing of the finite element analysis. The PATRAN program provides an interactive, graphics-oriented environment for creation of a geometric and finite-element model. A UDCPAT interface program reads the PATRAN generated neutral file for the model and generates a data file which may be used as inputs for the UDCFLOW finite element computer program. Simulation results from UDCFLOW runs may be transferred back to PATRAN for post-processing display. As an example, table 2 shows an example of the PATRAN command set which has been used to generate the cyclone model shown in figure 14.

TABLE 2

AN EXAMPLE OF PATRAN INTERACTIVE COMMANDS
FOR CYLONE MODEL GENERATION

```
START:
PATRAN
GO

PHASE I--GENERATE GEOMETRICAL MODEL:
GR,1,,0
GR,4,TR,12,1
GR,2/3,TR,0/10,1/4
LI,1/2,ST,,1/4,2/3
PA,1,2L,,1,2
SET,LINES,0
SET,CPLOT,ON
PA,A,REV
```

(Table 2 Continued)

```
PA,1,LAB,,1/2

PHASE II--GENERATE ANALYTICAL MODEL:
GF,P1,G,25/21
CF,PA,QUAD
DF,P1,DIS,3/0/0/0/0/0,1
DF,P1,FORC,3/0/0/0/0/1,1,ED1T4
SET,LABELS,OFF
PM,1,TAN,1,10000,1,0,4(0)
PM,2,TAN,6(0.025),1000,0.5
PM,3,TAN,0,0.018,2,2,0.005,3(0)
PM,4,TAN,3(5),3,2(0),100000,30

PHASE III--CREATE NEUTRAL FILE:
INTERFACE
NEUTRAL FILE
CREATE OUTPUT
ENTIRE FILE
OUTPUT FILE
OUTPUT PHASE I,YES
OUTPUT PHASE II,YES
NEUTRAL FILE PATRAN.OUT CREATED
STOP PATRAN

PHASE IV--TRANSLATE NEUTRAL FILE AND UDCFLOW RUN:
RUN PATUDC
RUN UDCFLOW

PHASE V--POST-PROCESSING DISPLAY:
RESTART PATRAN
OUTPUT RESULTS
USE EXTERNAL DATA FILE
VECTOR PLOT
USE DATA OTHER THEN INDICATED
PLOT RESULTANTS
COMPONENTS 1 AND 2
USE UDCFLOW OUTPUT FILE RESULT.DAT
PLOT MODEL
PLOT GRAPHS
```

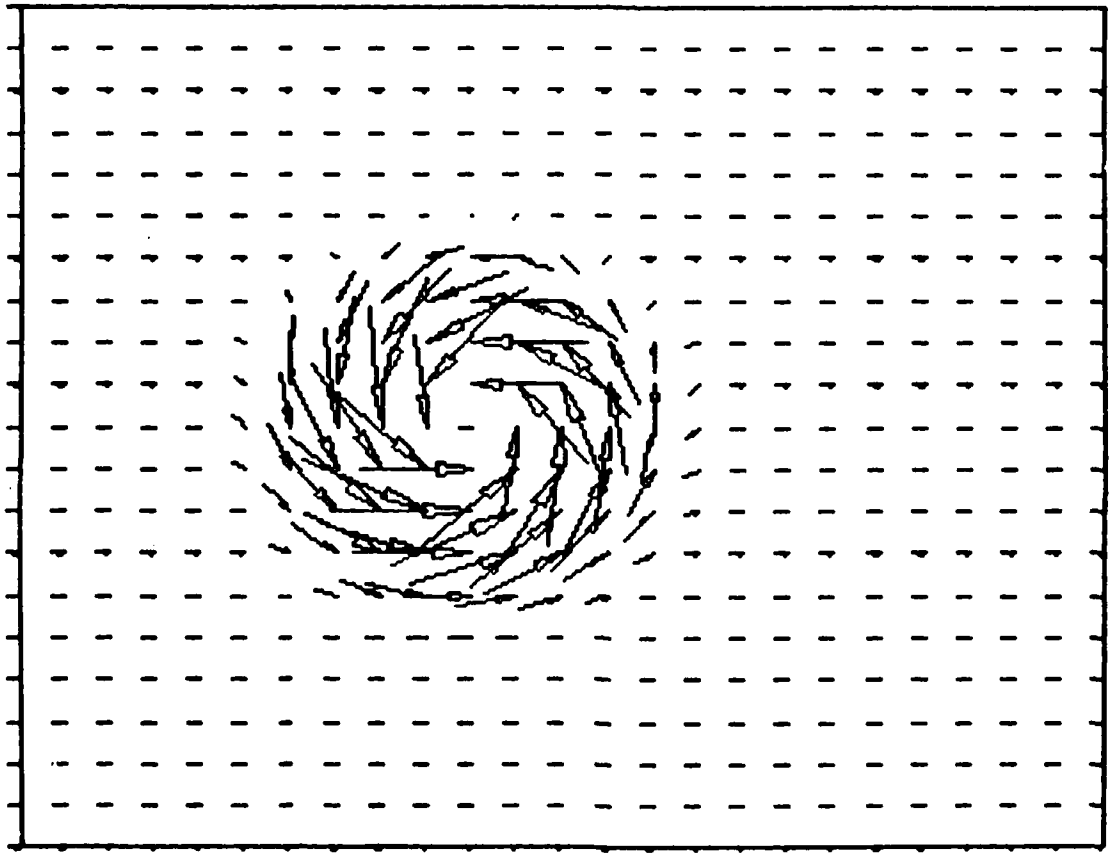

FIGURE 14 AN EXAMPLE OF A CYCLONE MODEL GENERATED BY PATRAN PRE-PROCESSOR

5. Results and Discussion

The algorithm developed can theoretically be used to simulate the two-dimensional atmospheric vortex. However, because of the vortex scale in nature, supercomputer will be required to simulate the atmospheric vortices. The author has so far used only the UDC's VAX-8650 computer for test runs of the program UDCFLOW. Several test runs have been made for problems of academic interests. Runs were first made for the one-dimensional fluid flow and thermal diffusion problems. Several examples of these runs have been presented and discussed in a paper by Chi, Berhanu and Ranje (1989) and a reprint of the report is appended to the report (see Appendix B).

A very popular two-dimensional flow problem is the so-called driven cavity, e.g., see Bozeman and Dalton (1973), Kawahara and Okamota (1976), and Baker (1983). Figure 15 shows a sketch of the driven cavity with the nondimensional lenct· by height being one by one. The cavity fluid is initially at rest, and the top lid of the cavity is started impulsively with a velocity which is used as the reference velocity v_r. Reynolds number for the cavity flow which is defined as $(v_r \ell_r / \nu_t)$ is assumed to be 100. At the test run, the flow domain is divided into a mesh of 20x20. Figures 16 through 20 show snapshots of the flow field at the nondimensional time (τ) equal to 0.0, 0.4, 1.0, 3.0 and 5.0, respectively. It can be seen in these figures that as time τ advances from 0 to 3 penetration of the flow depth increases. As time advances further from τ equal to 3, there is little change in the cavity flow. That is, steady state of the flow has been approached at τ equal to 3.

In conclusion, a general finite element computer program UDCFLOW has been developed to simulate transient flow develpment in the two-dimensional domain. The program has been integrated with the PDA's graphics-oriented PATRAN software package for finite-element analyses pre- and post-processing.

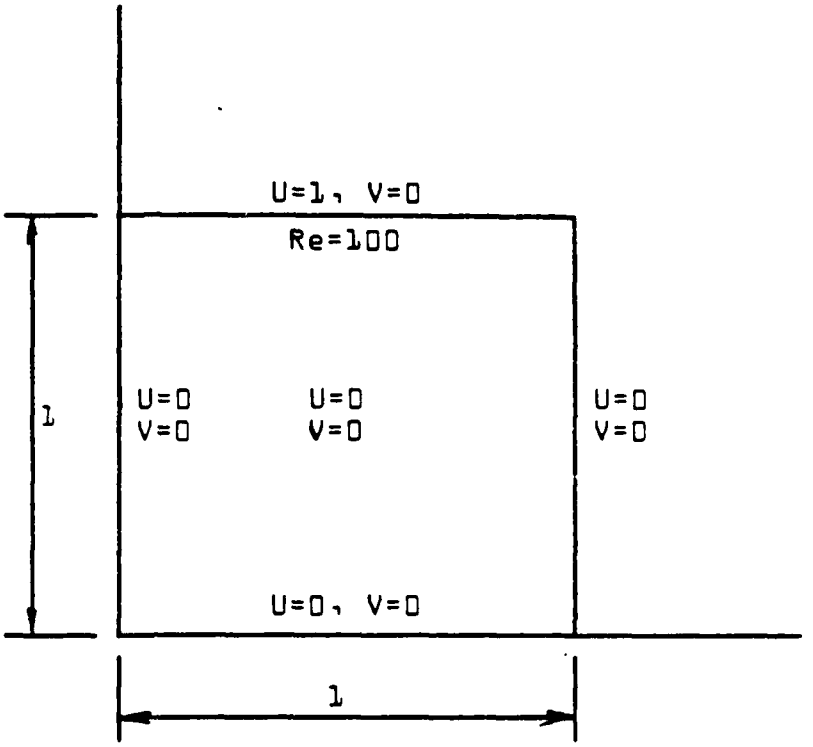

FIGURE 15 SCHEMATIC DIAGRAM OF A DRIVEN CAVITY SHOWING INTIAL AND BOUNDARY CONDITIONS

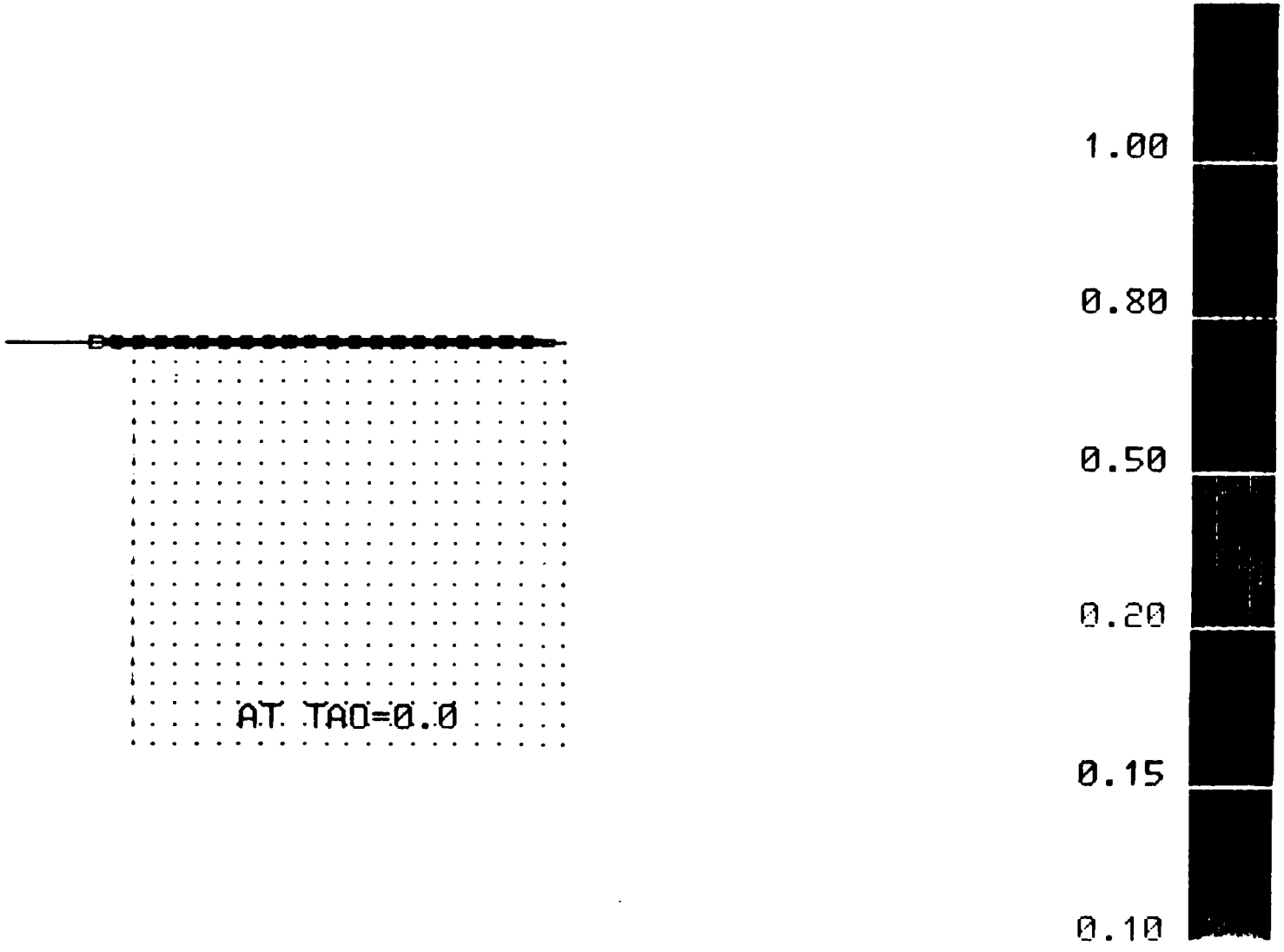

FIGURE 16 DRIVEN CAVITY SOLUTION AT RE=100 AND TAO=0.0

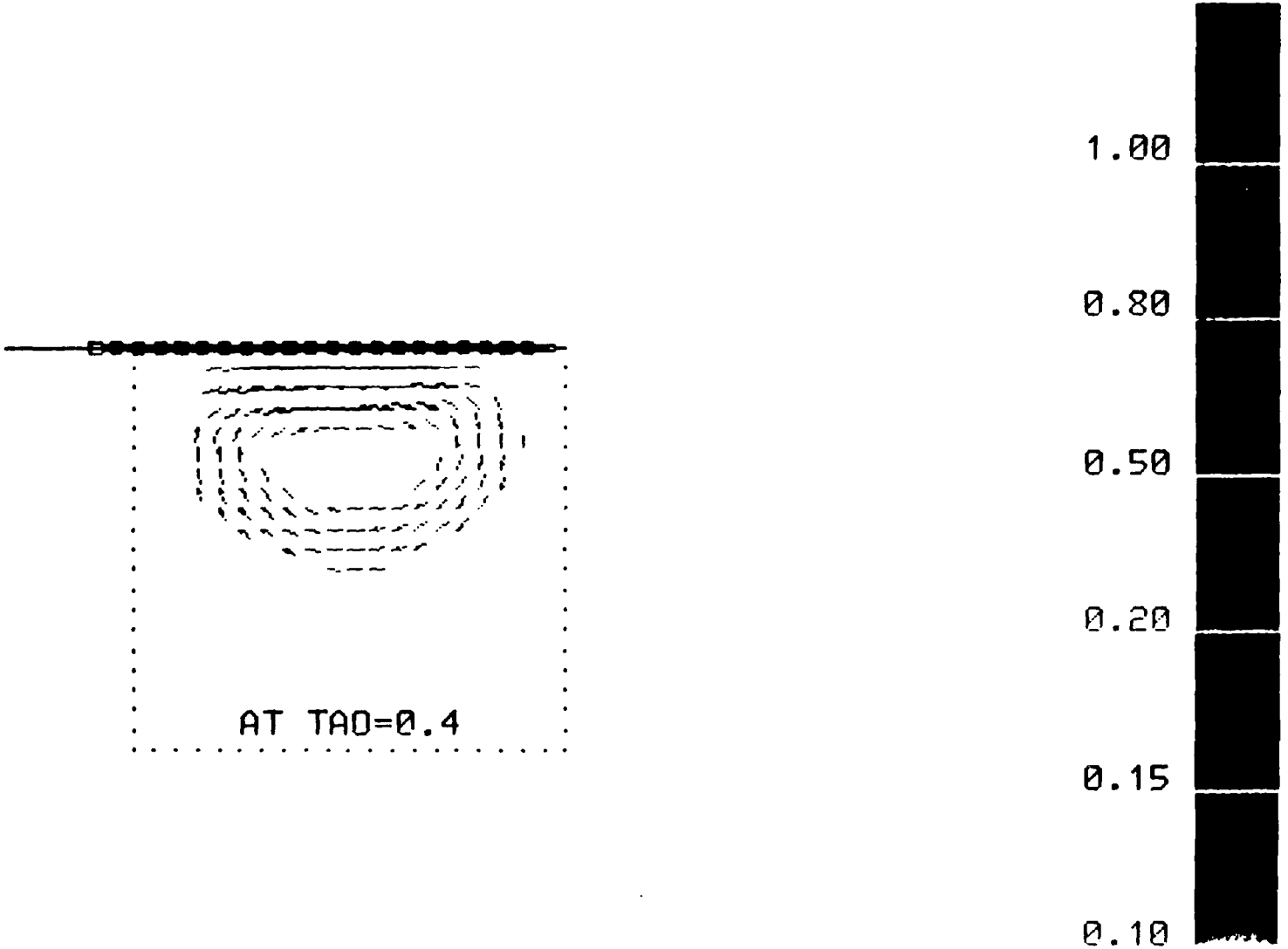

FIGURE 17 DRIVEN CAVITY SOLUTION AT RE=100 AND TAO=0.4

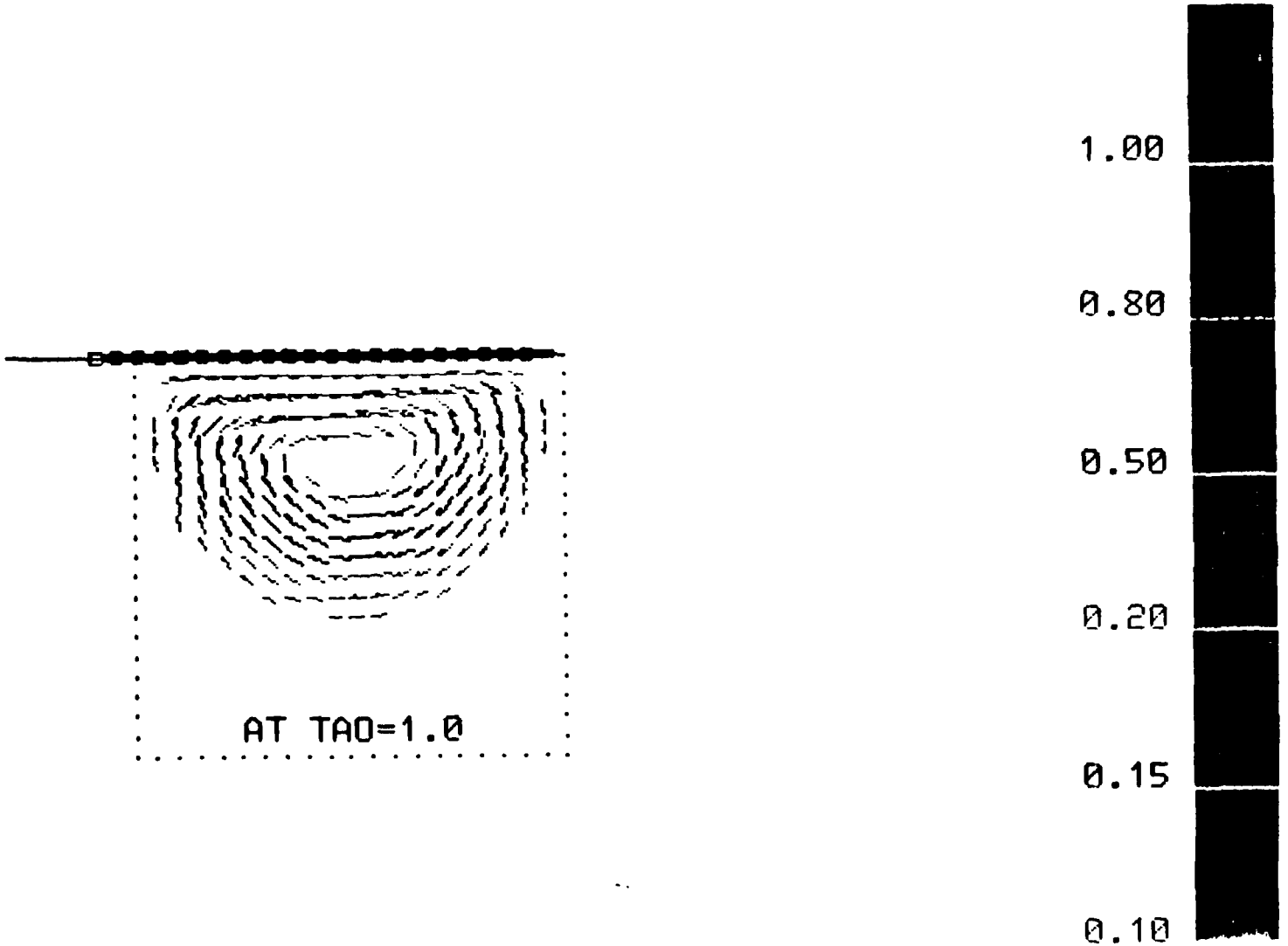

FIGURE 18 DRIVEN CAVITY SOLUTION AT RE=100 AND TAO=1.0

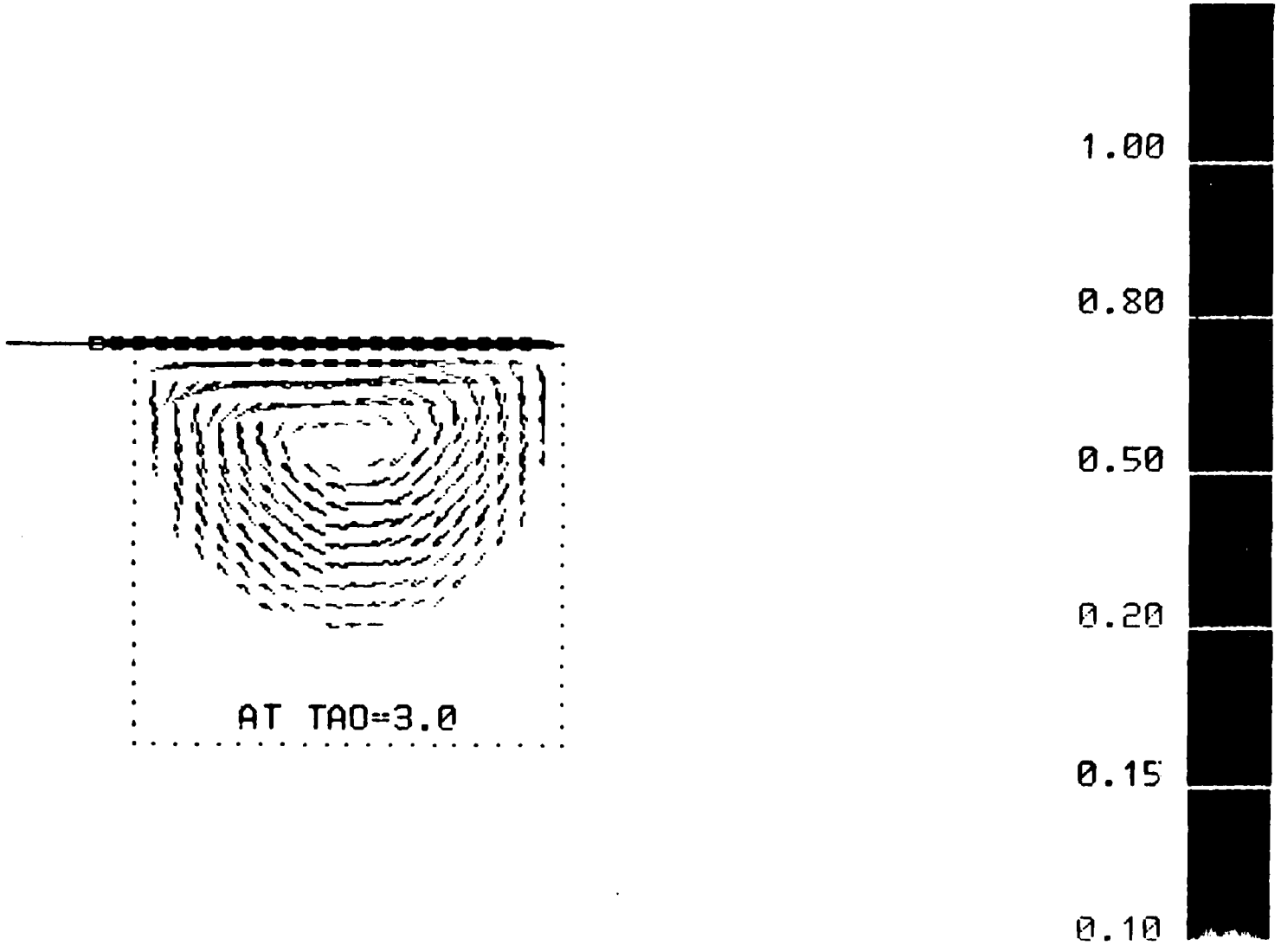

FIGURE 19 DRIVEN CAVITY SOLUTION AT RE=100 AND TAO=3.0

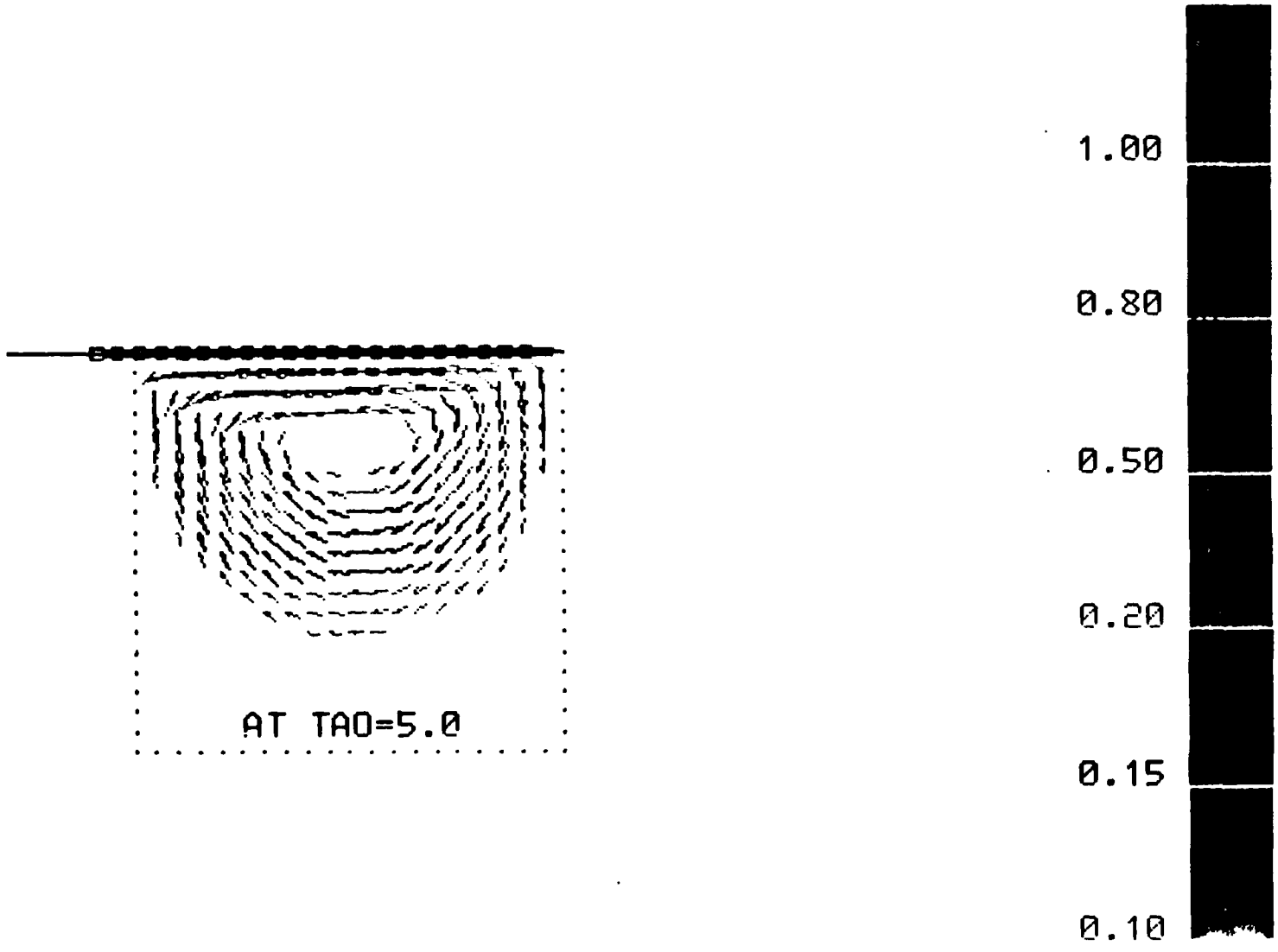

FIGURE 20 DRIVEN CAVITY SOLUTION AT RE=100 AND TA0=5.0

Runs of the program for several interesting problems have been made by the author and his co-workers. Effort is now being made by the author for accessing to Super-Computers to test applicability of the program to full-scale tropical cyclones in atmospheres.

6. CONCLUSIONS

Under the ONR Research Grant No. N00014-84-0610, UDC has undertaken a basic research on dynamics of marine atmospheres in tropical cyclones with an objective of improving understanding of turbulence in tropical cyclones and efficiency of computer simulation of tropical cyclones. For this objective, UDC has performed the following four phases of effort:

I. Development of mathematical models for marine planetary boundary layers of tropical cyclones over the sea surface.

II. Simulation of marine planetary boundary layers of tropical cyclones over the sea surface.

III. Tests in laboratory of air vortex flows over the water surface.

IV. Development of finite element computer programs for simulating marine planetary boundary layers of tropical cyclones.

Through these phases of effort, several accomplishments have been made. A turbulent theory for processes of the transport of heat, moisture and momentum in the marine planetary boundary layer has been developed. The theory uses the second-order turbulent closure model and calculates the turbulent stress components, and enthalpy and moisture fluxes. In addition, a simplified k-ε turbulent model is derived from the detailed turbulent flux model to increase the calculation efficiency. A computer program based upon the finite-difference numerical procedure has been coded to calculate the turbulent transport of heat, moisture and momentum in the marine planetary boundary layer of tropical cyclones.

To increase confidence in turbulence models and computer simulation, a vortex chamber with air/water interface has been designed and set up in

the UDC laboratory. The chamber has been instrumented with both the hot-film and laser doppler velocimeter. Tests have so far been made only with the hot-film anemometer and with air/solid-wall interface, and data from these tests with both the smooth and rough solid walls are in excellent agreement with the computer simulation results.

To increase simulation efficiency, a major effort has been made in development of a graphics-oriented interactive finite-element model for simulating transfer of heat, moisture and momentum in vortex flows. A finite-element analysis computer program (UDCFLOW) has been developed at UDC. Solutions have so far been obtained for transient one-dimensional heat and momentum transfer and two-dimensional momentun transfer equations. In addition, the UDCFLOW program has been integrated with the PDA's graphics-oriented PATRAN software package for finite-element analysis pre- and post-processing. Successful runs of the program for several interesting problems have been made by the author and his co-workers. Extension of runs to problems of vortex flow in marine atmospheres will need more extensive computer facility than the VAX-8650 which the author has been using. Effort is now being made by the author to access to "Super-Computers" to test applicabiliy of the program to study full-scale tropical cyclones in marine atmospheres. In addition, investigations are being made of possible permatations of index structure for the large-scale Jacobian metrices so as to decrease the central memory requirements for the Jacobians and to reduce the CPU time for their evaluation.

7. REFERENCES

Baker, A. J., 1983: Finite Element Computational Fluid Mechanics, McGraw-Hill Book Company, 281-283.

Bozeman, J. D. and C. Dalton, 1973: Numerical Study of Viscosity in a Cavity, J. Comp. Phy., 12, 348-363.

Chi, J., 1986: Dynamics of Marine Atmospheres in Tropical Cyclones. UDC Final Report to ONR Under Grant No. N00014-84-K-0610/P0001.

Chi, J., 1987: Heat, Moisture and Momentum Transfer in Turbulent Vortex Flows Over the Water Surface. Proceedings of 1987 ASME/ JSME Thermal Engineering Joint Conference, 3, 627-633.

Chi, J., E. Berhanu and M. H. Ranje, 1989: A Finite Element Computer Program for Dynamic Simulation of Thermal and Fluid Systems. Proceedings of 1989 ASEE Annual Conference, 2, 788-791.

Chou, P. Y., 1945: On Velocity Correlation and the Solution of the Equation of Turbulent Fluctuations. Qaurt. Appl. Mech., 3, 38-49.

Harlow, F. H. and C. W. Hirt, 1969: Generalized Transport Equations of Anisotropic Turbulence. Los Alamos Sci. Lab. Rept. No. LA-4086.

Kawahara, M. and T. Okamato, 1976: Finite Element Analysis of Steady Flow of Viscous Fluid Using Stream Function, Proc. ASCE, 47, 123-135.

Lewellen, W. S., 1981: Modeling the Lowest 1 km of the Atmosphere. North Atlantic Treaty Organization, Rept. No. AGARD-AG-267.

Launder, B. E., G. J. Reece and W. Rodi, 1975: Progress in Development of a Reynolds Stress Turbulence Closure. J. Fluid Mech., 68, 537-566.

Mellor, L. G. and T. Yamada, 1974: A Hierarchy of Turbulent Closure Models for Planetary Boundary Layers. J. Atmos. Sci., 31, 1860-1891.

Lumley, J. L. and G. R. Newman, 1977: The Return to Isotropy of Homo-Geneous Trubulence. J. Fluid Mech., 82, 161-175.

APPENDIX A--REPRINT OF A 1987 PAPER

Chi, J., 1987: Heat, Moisture and Momentum Transfer In Turbulent Vortex Flows Over The Water Surface, Proc. 1987 ASME/JSME Thermal Engineering Joint Conference, 3, 627-633.

HEAT, MOISTURE AND MOMENTUM TRANSFER IN TURBULENT VORTEX FLOWS OVER THE WATER SURFACE

J. Chi, Professor of Mechanical Engineering
University of the District of Columbia
Washington, D.C.

1987 ASME•JSME Thermal Engineering Joint Conference

March 22~27, 1987

Honolulu, Hawaii

THE JAPAN SOCIETY OF MECHANICAL ENGINEERS
SANSHIN HOKUSEI BUILDING 4-9
YOYOGI 2-CHOME, SHIBUYA-KU
TOKYO, 151 JAPAN

THE AMERICAN SOCIETY OF MECHANICAL ENGINEERS
UNITED ENGINEERING CENTER
345 EAST 47TH STREET
NEW YORK, NEW YORK 10017 U.S.A.

HEAT, MOISTURE AND MOMENTUM TRANSFER IN TURBULENT VORTEX FLOWS OVER THE WATER SURFACE

J. Chi, Professor of Mechanical Engineering
University of the District of Columbia
Washington, D.C.

ABSTRACT

This paper presents a numerical simulation of turbulent vortex boundary layers on the water surface. The model of turbulence employed is one that the turbulence energy and its dissipation rate are calculated by way of transport equations which are solved simultaneously with the vortex boundary layer mean flow equations for conservations of mass, momentum, energy and moisture. The model considered includes influences of the buoyancy, Coriolis and centrifugal forces, the air/water interface roughness, and the interface water droplet entrainment. Although lack of turbulence measurements over the water surface prevents a comlete comparison of the present theory with experiments, good agreement is obtained with available experimental data for the vortex boundary layer over simulated water surfaces.

NOMENCLATURE

C_p = constant pressure specific heat

C_z = a constant in equation for calculating the water surface roughness

f = Coriolis parameter

g = gravitational acceleration

H = mean moist specific enthalpy defined as $(S+Q_v)$

H_* = surface moist static energy flux

k = turbulence kinetic energy

L = water latent heat of vaporization

Q = mean total moisture mixing ratio defined as $(Q_\ell+Q_v)$

Q_ℓ = liquid water mixing ratio

Q_v = water vapor mixing ratio

Q_* = surface total moisture flux

r = radial distance

Ri = Richardson number

S = mean dry specific enthalpy defined as $C_p[T-(T_\circ-gz/C_p)]$

S_v = virtual dry specific enthalpy defined as $S(1+1.609Q_v-Q)$

T = temperature

$T_\circ$ = standard temperature

U = mean velocity component in radial direction

U_* = surface frictional velocity

V = mean velocity component in tangential direction

V_m = mean tangential velocity at the vortex outside radius

W = mean velocity component in vertical axial direction

X = dependent variables

z = vertical axial distance

$z_\circ$ = water surface roughness length

z_1 = first layer of air next to the air/water interface

α = a coefficient in finite difference equations

β = expansion coefficient or a coefficient in finite difference equations

θ = a function of Richardson number defined in text

γ = a quantity defined as $(L/C_p)(\partial Q_g/\partial T_g)$ or a coefficient in finite difference equations

δ = a coefficient in finite difference equations

Δ = boundary layer thickness

ε = turbulence energy dissipation rate

ζ = a quantity defined as $C_p T_\phi / L$

ϕ = azimuth angle

ν_t = turbulent kinematic viscosity

σ = Prandtl/Schmidt number for turbulent diffusion

Ψ = a function of Richardson number defined in text

SUBSCRIPTS

g = saturated vapor

h = pertaining to diffusional transport of moist specific enthalpy

k = pertaining to diffusional transport of turbulence energy

m = values of the radial position where the main vortex tangential velocity is maximum or the vertical grid position in a finite difference scheme

M = grid position at the vortex top boundary

n = the horizontal grid position in a finite difference scheme

N = grid position at the vortex outside radius

q = pertaining to diffusional transport of moisture

s = pertaining to diffusional transport of dry specific enthalpy

x = pertaining to the dependent variable X

ε = pertaining to diffusional transport of turbulence dissipation rate

* = lower boundary of an air vortex at the air/water interface

1 = air layer next to the air/water interface

- = outside radial boundary of an air vortex

+ = top boundary of an air vortex

INTRODUCTION

In their earlier papers, the present author and his co-workers reported several numerical simulation results for the turbulent vortex boundary layer on smooth solid surfaces, using the Karman's integral method [1]. The mixing length theory [2], and the turbulent energy method [3], respectively. Recent advances in turbulence modeling and numerical methods (e.g., see Harlow and Hirt[4], Gibson and Spalding [5], Hanjalic and Launder [6], Mellor and Yamada [7], Lewellen [8], and Chi [9]) have made it a common practice to solve simultaneously transport equations for turbulence quantities with conservation equations for mean flows. Many parameters for complex turbulent flows can now be simulated by numerical methods. In this paper, the author presents a numerical simulation of turbulent vortex boundary layer flows over the water surface like that shown in Fig. 1.

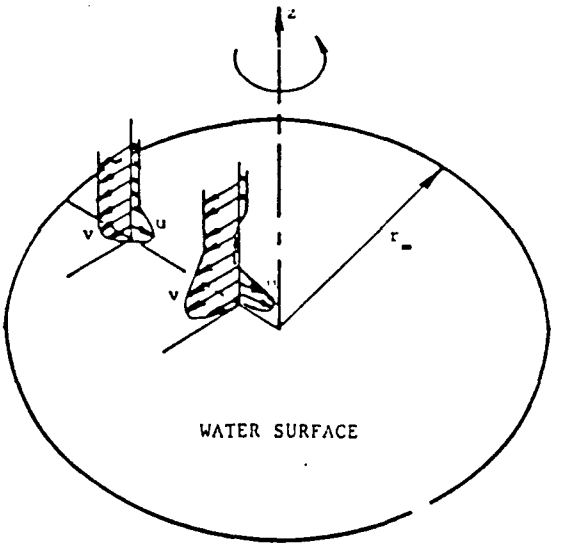

Fig. 1 Sketch of the Vortex Flow Over a Water Surface

The flow situation shown in Fig. 1 occurs in natural atmospheres such as the marine planetary boundary layer of tropical cyclones as well as engineering devices such as wet cyclones and thermal processors. It presents many challenging problems which are of interests to researchers in areas of heat and mass transfer, fluid dynamics and marine meteorology. These problems include the boundary layer heat, moisture and momentum transfer; turbulence production, dissipation and diffusion; strong influence of the gravitational, Coriolis and centrifugal forces; and influence of air-water interface roughness and liquid droplet entrainment.

The model of turbulence employed in this paper is one which calculates the turbulent kinetic energy k and its dissipation rate ε by way of their transport equations. The turbulent kinematic viscosity will be calculated from k and ε values [10],

$$\nu_t = 0.09k^2/\varepsilon \qquad (1)$$

Mean conservation equations which will be solved simultaneously are those not only for balances of mass and momentum but also for balances of the moist static energy and the total moisture mixing ratio so as to enable the model to simulate both the air/water interface evaporation and the interface water droplet entrainment. The Coriolis force due to earth rotation and the centrifugal force due to the flow circulation are included in formulating the model momentum balance. Influences of buoyancy force and surface roughness are accounted for in formulating the model turbulence

[1] The number in brackets refer to the references at the end of the paper

transportation and the model flow boundary conditions.

In subsequent two sections of this report, governing equations for the model are derived along with their relevant initial and boundary conditions and their solution procedure; and results are presented and discussed.

THE MODEL

Governing Equations

Coordinates are chosen so that z axis is vertical, r axis is in the radial direction and ϕ is the azimuth angle. When the Boussinesq and boundary layer approximations and the axisymmetrical and quasi-steady flow assumptions are used, governing equations for conservations of mean mass, mean motion radial-direction momentum, mean motion tangential-direction momentum, mean motion moist static energy, mean motion total moisture mixing ratio, mean turbulence kinetic energy and mean turbulence dissipation rate become

$$\frac{\partial Ur}{r\partial r} + \frac{\partial W}{\partial z} = 0 \tag{2}$$

$$U\frac{\partial U}{\partial r} + W\frac{\partial U}{\partial z} = [(f+\frac{V}{r})V - (f+\frac{V_\infty}{r})V_\infty] + \frac{\partial}{\partial z}(\nu_t\frac{\partial U}{\partial z}) \tag{3}$$

$$U\frac{\partial V}{\partial r} + W\frac{\partial V}{\partial z} = -(f+\frac{V}{r})U + \frac{\partial}{\partial z}(\nu_t\frac{\partial V}{\partial z}) \tag{4}$$

$$U\frac{\partial H}{\partial r} + W\frac{\partial H}{\partial z} = \frac{\partial}{\partial z}(\frac{\nu_t}{\sigma_h}\frac{\partial H}{\partial z}) \tag{5}$$

$$U\frac{\partial Q}{\partial r} + W\frac{\partial Q}{\partial z} = \frac{\partial}{\partial z}(\frac{\nu_t}{\sigma_q}\frac{\partial Q}{\partial z}) \tag{6}$$

$$U\frac{\partial k}{\partial r} + W\frac{\partial k}{\partial z} = \frac{\partial}{\partial z}(\frac{\nu_t}{\sigma_k}\frac{\partial k}{\partial z}) + \nu_t[(\frac{\partial U}{\partial z})^2 + (\frac{\partial V}{\partial z})^2 - \frac{\beta g}{\sigma_s}\frac{\partial S_v}{\partial z}] - \epsilon \tag{7}$$

$$U\frac{\partial \epsilon}{\partial r} + W\frac{\partial \epsilon}{\partial z} = \frac{\partial}{\partial z}(\frac{\nu_t}{\sigma_\epsilon}\frac{\partial \epsilon}{\partial z}) + 1.45\frac{\epsilon}{k}\nu_t[(\frac{\partial U}{\partial z})^2 + (\frac{\partial V}{\partial z})^2 - \frac{\beta g}{\sigma_s}\frac{\partial S_v}{\partial z}] - 2\frac{\epsilon^2}{k} \tag{8}$$

In the above equations, U, V and W are the mean velocity components in the r, ϕ and z directions; and H is the mean moist specific enthalpy, Q the mean total moisture mixing ratio, k the mean turbulence kinetic energy and ϵ the mean turbulence energy dissipation rate. The turbulent viscosity appearing in the diffusion term is calculated by equation (1). The turbulent exchange coefficients for diffusions of the moist static energy, the total moisture ratio, the virtual dry specific enthalpy, the turbulence kinetic energy and the turbulence dissipation rate are related to the turbulent viscosity through the turbulent Prandtl-Schmidt numbers which are all supposed to take on the following constant values:

$$(\sigma_h, \sigma_q, \sigma_s, \sigma_k, \sigma_\epsilon) = (0.9, 0.9, 0.9, 1.0, 1.3) \tag{9}$$

In the above equation set, the turbulence stresses and fluxes have been modeled by the expression $[(\nu_t/\sigma_x)(\partial X/\partial z)]$ in which X represents any mean quantity of a dependent variable value. Values of $[(\nu_t/\sigma_x)(\partial X/\partial z)]$ in equations (2) through (8) can be calculated from the predicted X distributions. However, the buoyancy terms in equations (7) and (8) contain a derivative of S_v which is not one of the directly predicted variables. In order to relate $(\partial S_v/\partial z)$ to the predicted variables H and Q, we follow a derivation discussed by Moeng and Arakawa [11], which yields the following relationships:

$$\frac{\partial S_v}{\partial z} = \sigma_s[\frac{\partial H}{\sigma_h\partial z} + \frac{(0.609\zeta - 1)L\partial Q}{\sigma_q\partial z}] \quad \text{(for clear region)} \tag{10}$$

$$\frac{\partial S_v}{\partial z} = \sigma_s[\frac{(1+1.609\zeta\gamma)\partial H}{(1+\gamma)\sigma_h\partial z} - \frac{\zeta L\partial Q}{\sigma_q\partial z}] \quad \text{(for cloudy region)} \tag{11}$$

Here γ is equal to $(L/C_p)(\partial Q_g/\partial T_g)$, ζ is equal to C_pT_o/L, and sufix g stands for the saturated water condition. Equations (2) through (8) together with the auxiliary functions discussed above now form a model for turbulent vortex flows over the water surface. In addition, the boundary layer model requires specification of initial conditions and boundary values at the edges of the flow.

Bottom Boundary Conditions

At the air/water interface, both the water surface roughness and the surface layer stability influence the air vortex bottom boundary conditions. The water surface roughness length can be calculated by the equation [12]:

$$z_o = C_z U_*^2/g \tag{12}$$

where U_* is the surface frictional velocity, g the gravitational acceleration, C_z a constant whose value depends on the extent of the flow field. For example, for the air/sea interface it is equal to 1.6×10^{-2}, for the laboratory wave channel [12] it is equal to 1.12×10^{-2}, and for the UDC vortex chamber [9] which will be discussed later in the paper it is equal to 5.58×10^{-3}.

For numerical modeling, the boundary layer in the vortex flow is divided into horizontal layers and concentric cylindrical surfaces. The first bottom layer will be at a height $z=z_1$. U, V, H and Q values at the surface layer can be calculated by the equations [13,14]:

$$(U_1^2 + V_1^2)^{\frac{1}{2}} = 2.50U_*[\ln(\frac{z_1}{z_o}) + \Psi(Ri_1)] \tag{13}$$

$$(H_1 - H_o) = 1.85H_*[\ln(\frac{z_1}{z_o}) + \Theta(Ri_1)] \tag{14}$$

$$(Q_1 - Q_o) = 1.85Q_*[\ln(\frac{z_1}{z_o}) + \Theta(Ri_1)] \tag{15}$$

Here U_*, H_* and Q_* are the surface frictional velocity, the surface moist static energy flux, and the surface total moisture flux, respectively; and the Richardson number Ri is defined as follows:

$$Ri = [0.4g(\frac{\nu_t}{\sigma_s})(\frac{\partial S_v}{\partial z})_z]/(U_*^2 S_v) \tag{16}$$

The stability functions $\Psi(Ri)$ and $\Theta(Ri)$ are calculated by the equations:

$$\Psi(Ri) = 4.7Ri \quad [\text{for } Ri \geq 1]$$
$$= -\ln(0.5[1+(1-15Ri)^{\frac{1}{2}}]) - 2\ln(0.5[1+(1-15Ri)^{\frac{1}{2}}]) + 2\tan^{-1}(1-15Ri)^{\frac{1}{2}} - 0.5\pi \quad [\text{for } Ri \leq 1] \tag{17}$$

$$\theta(Ri) = 6.35Ri \qquad [\text{for } Ri \geq 1]$$
$$= -21\ln(0.5[1+(1-9Ri)^{\frac{1}{2}}]) \qquad [\text{for } Ri \leq 1] \qquad (18)$$

k and ε values at the bottom boundary layer can be calculated by the equations [15]:

$$k = 3.33U_*^2(1+4.7Ri_1)^{-2} \qquad [\text{for } Ri \geq 1]$$
$$= 3.33U_*^2(1-15Ri_1)^{\frac{1}{2}} \qquad [\text{for } Ri \leq 1] \qquad (19)$$

$$\varepsilon = 0.412k^{3/2}z_1^{-1} \qquad (20)$$

Top Boundary Conditions

Mean velocity components for the main vortex flow at $z=z_+$ and all r have been calculated by numerous workers, e.g., see Root[16], Sullivan [17] and Lewellen [18]. The result can be represented accurately by the equations:

$$U_+ = \frac{(U_+)_-(r_-)}{r}\left(1 - \exp\left[-\frac{2.506\nu_t}{(U_+)_-r_-}\left(\frac{r}{r_m}\right)^2\right]\right) \qquad (21)$$

$$V_+ = \frac{1.4V_m r_m}{r}\left(1 - \exp\left[-1.253\left(\frac{r}{r_m}\right)^2\right]\right) \qquad (22)$$

where suffix + represents values at the top boundary, suffix − represents values at large radius, and suffix m represents values at a position in the main flow where the vortex tangential velocity is maximum. In the main flow, the mean moist static energy H and the mean total moisture ratio Q values are expected to be linear with respect to z. Hence their top boundary conditions are as follows:

$$\frac{\partial^2 H}{\partial z^2} = 0 \qquad (23)$$

$$\frac{\partial^2 Q}{\partial z^2} = 0 \qquad (24)$$

The values of k and ε at the top boundary can be determined from the degenerative forms of equations (7) and (8) which result when gradients with respect to z are set to zero. That is,

$$\frac{\partial k}{\partial r} = -\frac{\varepsilon_+}{U_+} \qquad (25)$$

$$\frac{\partial \varepsilon}{\partial r} = -\frac{2(\varepsilon_+)^2}{(U_+)(k_+)} \qquad (26)$$

Side Initial Values

For the side boundary initial values, the boundary thickness Δ, the radial velocity amplitude value E and the surface frictional velocity U at the outside radius $r = r_-$ may first be calculated by a Karman's integral method [1]. Initial values for U, V, H and Q at $r=r_-$ and all z can then be represented by the following functions [1,14]:

$$V = \frac{2.5U_*}{(1+E^2)^{\frac{1}{2}}}\left[\ln\left(\frac{z}{z_0}\right) + \Psi(Ri)\right] \qquad (27)$$

$$U = EV(\tfrac{1}{2}[1+\cos(\tfrac{\pi z}{\Delta})])(1 - 2[1 - \frac{(U_+)_-}{E(V_+)_-}](\frac{z}{\Delta}) + [1 - \frac{(U_+)_-}{E(V_+)_-}](\frac{z}{z_0})^2) \qquad (28)$$

$$H - H_0 = 1.85H_*[\ln(\frac{z}{z_0}) + \theta(Ri)] \qquad (29)$$

$$Q - Q_0 = 1.85Q_*[\ln(\frac{z}{z_0}) + \theta(Ri)] \qquad (30)$$

Here Ri, Ψ and θ values are determined by equations (16) through (18), respectively. The side turbulence energy profile may be represented by the polynomial [19]:

$$k = ((k_1)_-/[1 - 2(\tfrac{z}{\Delta})^2 + 3(\tfrac{z}{\Delta})^3])[1-2(\tfrac{z}{\Delta})^2+3(\tfrac{z}{\Delta})^3] \qquad (31)$$

in which $(k_1)_-$ is the bottom boundary turbulence energy value at $r=r_-$. It can be calculated by equation (19). Value for the side boundary turbulence dissipation rate is related to the turbulence energy value by the equation:

$$\varepsilon = 0.412k^{3/2}z^{-1} \qquad (32)$$

Solution Procedure

The conservation equations (3) through (8) for U, V, H, Q, k and ε have a parabolic form of

$$U\frac{\partial X}{\partial r} + W\frac{\partial X}{\partial z} = \frac{\partial}{\partial z}\left(\frac{\nu_t}{\sigma_x}\frac{\partial X}{\partial z}\right) + \text{Source} \qquad (33)$$

Several finite-difference methods of solution for equation (33) are available in the literature [20]. We have written a computer program following an extension of the implicit procedure given by Crank and Nicholson [21]. Using a rectangular grid system on the (r,z) plane with

$$r_{n+1} = r_n + \Delta r_n \qquad (n=1,2,\ldots,N)$$
$$z_{m+1} = z_m + \Delta z_m \qquad (m=1,2,\ldots,M) \qquad (34)$$

The equation set (33) for different quantities of the model independent variables are approximated at the point (r_{n+1}, z_m) and written in the form:

$$\alpha_m^n X_{m-1}^n + \beta_m^n X_m^n + \gamma_m^n X_{m+1}^n = \delta_m^n \qquad (35)$$

Here at n=N, values of X are equal to the side initial values at $r=r_-$; at m=1, values of X are equal to the bottom boundary values at $z=z_1$; and at m=M, values of X are equal to the top boundary values at $z=z_+$. Integrating equation (33) from n=N-1 with m from 1 to M, values of X_{N-1}^m with m from 1 to M can be determined. Value of n is then reduced by one to determine X_{N-2}^m. The process is continued, until it covers the whole (r,z) domain for the problem. Structural details of the program can be found in a paper by Chi and Glowacki [2].

RESULTS AND CONCLUSION

In order to establish confidence in the present model, some measurements of the turbulent vortex flow have recently been made (on a UDC vortex test chamber) by the author and a co-worker. Details of the experimental set-up (Fig. 2) were given by Chi and Hinds [9]. Briefly, the test chamber's overall dimension is 55-cm diameter by 90-cm high. It generates an air vortex of 30.48-cm diameter by 15-cm high. The vortex is generated by forcing air through 24 evenly spaced vanes of 15-cm high placed on a 30.48-cm diameter pitch circle. The swirling air discharges from the chamber through a 3.81-cm

diameter hole located at center of the chamber's top disk. Bottom of the swirling air is in contact with a pool of water which can be maintained at a constant depth and at desired temperatures. A scaled needle probe may be inserted vertically from the bottom into the chamber at different radial positions to measure mechanically the wave heights.

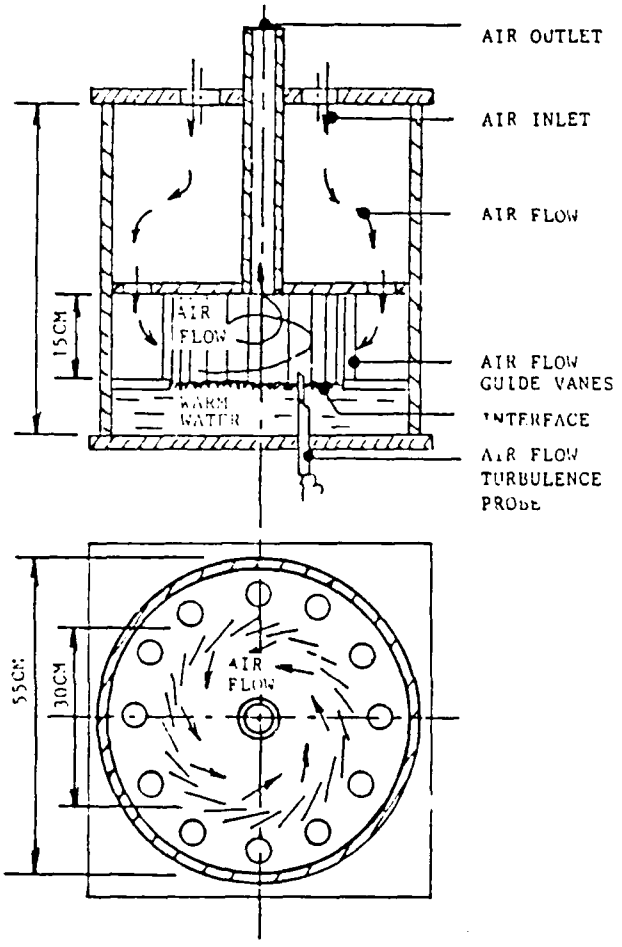

Fig. 2 Schematic of a Laboratory Vortex Chamber with Air/Water Interface

Because the chamber is not currently instrumented to compensate for influences of water entrainment on the air flow measurement, direct measurements of air velocity over the actual water surface have not been made. Solid surfaces of different roughness heights were used to simulate physically the air/water interface roughness. The horizontal component of velocity and its direction in the vicinity of the rough solid surface have been measured by a directionally sensitive wedge-shaped hot-film probe. The hot film was on the axis of the cylindrical stem of the probe, and the probe was traversed axially through the bottom plate at different radii so that the horizontal velocities at different radii and heights could be measured. Figures 3 and 4 show the measured vortex boundary layer velocity profiles, U and V, respectively, versus z at several radii and with the surface roughness values indicated.

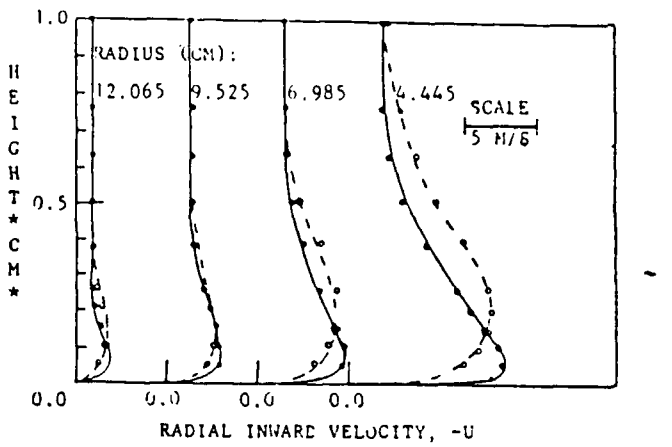

Fig 3 Predicted and Measured Radial Velocity on Solid Surface. (Keys: o & ——, Measured & Calculated values on Smooth Surface; o & ---, Measured & Calculated Values on Rough Surface of Sand Grain Mesh #120)

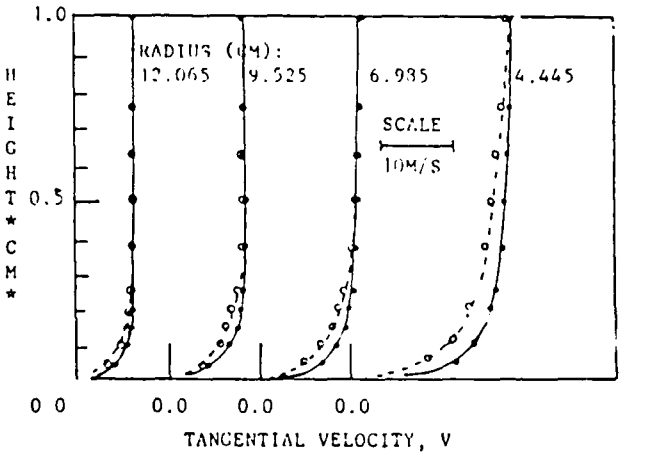

Fig. 4 Predicted and Measured Tangential Velocity on Solid Surface. (Keys: o & ——, Measured & Calculated Values on Smooth Surface; o & ---. Measured & Calculated Values on Rough Surface of Sand Grain Mesh #120)

As numerical examples, the computer program for the present model has been run to simulate the turbulent vortex boundary layer flows under the same main vortex conditions as in the experiments but with several different bottom surface conditions as follows:

1. Smooth solid surface,
2. Sand-roughness solid surface, and
3. Actual water surface.

For smooth solid surface calculations, z_o values were calculated from z_o equal to $0.111\nu/U_*$, and for sand roughness-surface calculations, z_o values were calculated from z_o equal to 1/30th of the sand grain height. Both of these relationships have been obtained from Schlichting [22]. The predicted radial velocity U and tangential velocity V over the smooth and rough surfaces are plotted versus z for several radii in Figs. 3 and 4 for comparison with the experiments. The ability of the present theory to correlate the measured mean velocity profiles in turbulent vortex boundary layers over smooth and rough solid surfaces is demonstrated in Figs.

3 and 4 by excellent agreement between the prediction and experiments.

In predicting the vortex boundary layer flow on the actual water surface, equation (12) was used to calculate the air/water interface roughness. Constant C_z for equation (12) was chosen to be 0.0558 so that the numerically simulated air/water interface roughness values z_o were in close agreement with the 1/30th of the measured water wave heights. Calculations have been made with the assumptions that the main vortex air is maintained at 20°C and 50% relative humidity (i.e., with H_∞=16.8 kJ/kg and Q_∞=0.007 kg/kg) and that air at the water surface is maintained at 25°C and 100% relative humidity (i.e., with H_o=53.0 kJ/kg and Q_o=0.020 kg/kg). Figs. 5 through 9 show plots of the calculated radial velocity, tangential circulating velocity, moist static specific enthalpy, total moisture ratio and turbulence energy profiles for the vortex flow over the actual water surface.

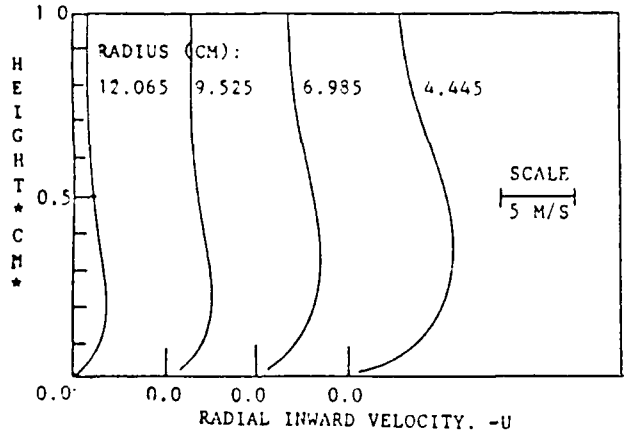

Fig. 5 Predicted Radial Velocity Over a Water Surface

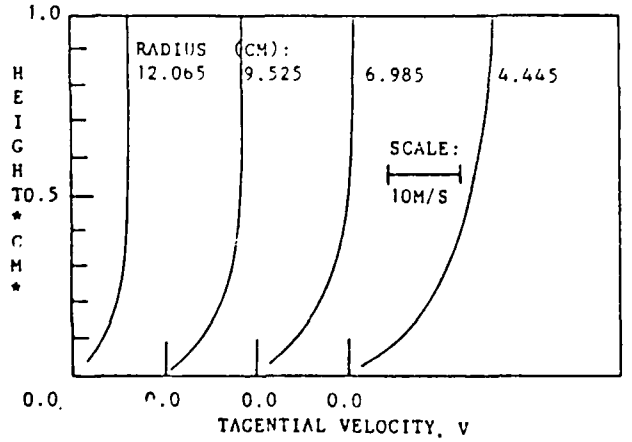

Fig. 6 Predicted Tangential Velocity Over a Water Surface

Many interesting characteristics for the vortex boundary layer flow can be observed from the above presented numerical simulations. Near the air/water interface, retardation of the tangential velocity is seen in Figs. 3 and 6. This retardation is accompanied by a reduction in the centrifugal force; the balance between pressure and the centrifugal force is thereby destroyed. The flow in this region is thus characterized by the entrainment of air from the main vortex into the boundary layer as indicated by an excess of the radial velocity inside the boundary layer over its value in the main vortex at the same radius. Effects of the solid surface roughness and the water surface waviness can be seen in Figs. 3, 4, 5 and 6 to increase the boundary layer thickness but to decrease the abruptness in deceleration of the tangential flow and in acceleration of

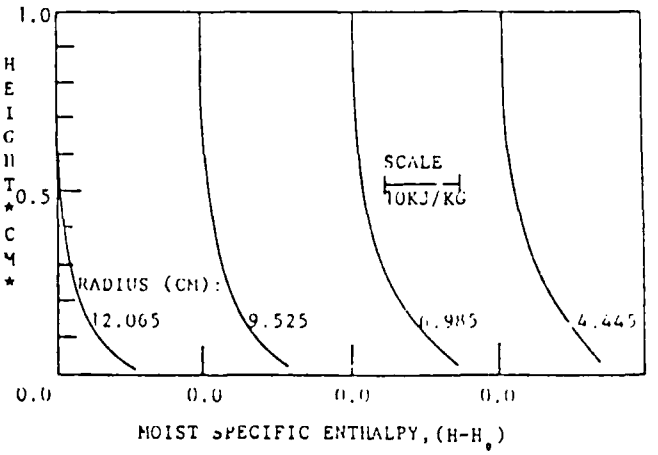

Fig. 7 Predicted Moist Specific Enthalpy Over a Water Surface

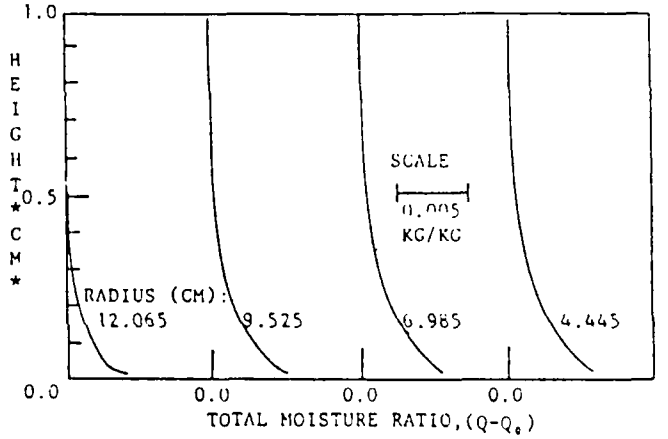

Fig. 8 Predicted Total Moisture Ratio Over a Water Surface

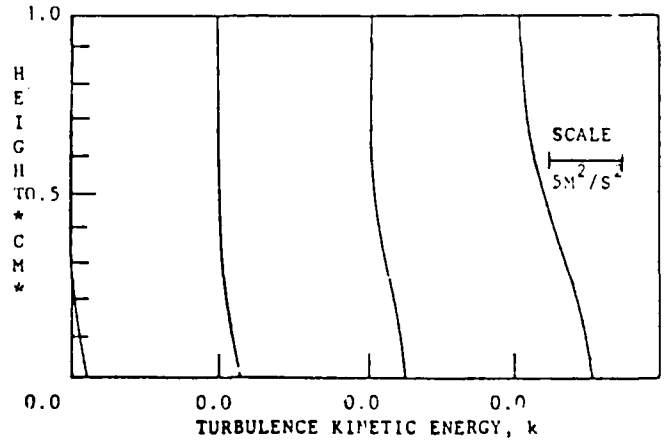

Fig. 9 Predicted Turbulent Kinetic Energy Over a Water Surface

the radial flow. In addition, the large radial inward velocity inside the vortex boundary layer carries circulation, static enthalpy, moisture content and turbulence energy from large radii to a position near the axis of symmetry as can be seen at small radius in Figures 5 and 6 of the large V, in Fig. 7 of the large $(H-H_s)$, in Fig. 8 of large $(Q-Q_s)$, and in Fig. 9 of the large k.

In conclusion, a numerical simulation of turbulent boundary layer flows on the water surface has been developed. The model of turbulence employed is one that the turbulence energy and its dissipation rate are calculated by way of transport equations which are solved simultaneously with the vortex boundary layer conservations of mass, momentum, moist static enthalpy and total moisture ratio for the mean motion. As far as possible, predicted flows are compared with available measured mean values in the vortex boundary layer. The ability of the present model to correlate the empirical data is shown to be good (see Figs. 3 and 4). In addition several interesting characteristics of turbulent vortex boundary layer flows over the water surface are predicted by the model. Predictions of the radial inward convergence of mass, circulation, enthalpy, moisture and turbulence energy from large radii to a position near the axis of symmetry are in agreement with the known physical laws.

ACKNOWLEDGEMENT

This work was supported by the Office of Naval Research. The author wishes to express his appreciation to the Office.

REFERENCES

1. Chi, S. W.[1], Ying, S. I. and Chang, C. C., "The Ground Turbulent Boundary Layer of a Stationary Tornado-Like Vortex," TELLUS, Vol. 21, 1969.

2. Chi, S. W., and Glowacki, W. J., "Applicability of Mixing Length Theory to Turbulent Boundary Layers Beneath Intense Vortices," J. Appl. Mech., Vol. 41, 1974.

3. Chi, J., "Numerical Analysis of Turbulent End-Wall Boundary Layers of Intense Vortices," J. Fluid Mech., Vol. 82, 1977.

4. Harlow, F. H. and Hirt, C. W., "Generalized Transport Equations of Anisotropic Turbulence," Los Alamos Sci. Lab., Rept. No. LA-4086, 1969.

5. Gibson, M. M. and Spalding, D. B., "A Two-Equation Model of Turbulence Applied to the Prediction of Heat and Mass Transfer in Wall Boundary Layers," ASME Paper No. 72-HT-15, 1972.

6. Hanjalic, K. and Launder, B. E., "Fully Developed Asymmetric Flow in a Plane Channel," J. Fluid Mech., Vol. 52, 1972.

7. Mellor, L. G. and Yamada, T., "A Hierachy of Turbulent Closure Models for Planetary Boundary Layers," J. Atmos. Sci., Vol. 31, 1974.

8. Lewellen, W. S., "Modeling the Lowest 1-km of the Atmosphere," North Atlantic Treaty Organization, Rept. No. AGARD-R-67, 1981.

9. Chi, J. and Hinds, G. B., "A Turbulence Theory for Vortex Marine Planetary Boundary Layers and Comparison with Experiments," University of the District of Columbia, Rept. No. MMEG-8511, 1985.

10. Jones, W. P. and Launder, B. E., "The Calculation of Low-Reynolds-Number Phenomena with a Two-Equation Model of Turbulence," ASME Paper No. 72-HT-20, 1972.

11. Moeng, C. H. and Arakawa, A., "A Numerical Study of a Marine Subtropical Stratus Layer and Its Stability," J. Atmos. Sci., Vol. 37, 1980.

12. Wu, J., "Laboratory Studies of Wind-Wave interactions," J. Fluid Mech., Vol. 34, 1968.

13. Paulson, C. A., "The Mathematical Representation of Wind Speed and Temperature Profiles in the Unstable Atmospheric Surface Layer," J. Appl. Meteor., 1970.

14. Deardorff, J. W., "Parameterization of the Planetary Boundary Layer for Use in General Circulation Models," Mon. Wea. Rev., Vol. 100, 1972.

15. Businger, J. A., Wynaard, J. C., Izumi, Y. and Bradley, E. F., "Flux-Profile Relationships in the Atmospheric Surface Layer," J. Atmos. Sci., Vol. 28, 1971.

16. Rott, N., "On the Viscous Core of a Line Vortex," ZAMM, Vol. 10, 1979.

17. Sullivan, R. D., "A Two-Cell Vortex Solution of the Navier-Stokes Equations," AIAA Journal, Vol. 26, 1959.

18. Lewellen, W. S., "A Solution for Three-Dimensional Vortex Flow with Strong Circulation," J. Fluid Mech., Vol. 14, 1962.

19. Chi, S. W. and Chang, C. C., "Effective Viscosity in a Turbulent Boundaly Layer," AIAA Journal, Vol. 7, 1969.

20. Ames, W. F., "Nonlinear Partial Differential Equations in Engineering," Academic Press, New York, NY, 1965.

21. Crank, J. and Nicholson, P., "A Practical Method for Numerical Evaluation of Solutions of Partial Differential Equations for the Heat Conductions Type," Proc. Camb. Phil. Soc., Vol. 43, 1947.

22. Schlichting, H., "Boundary Layer Theory," McGraw-Hill, New York, NY, 1960.

[1]The author's name has since 1977 been changed to J. Chi

APPENDIX B--REPRINT OF A 1989 PAPER

Chi, J., E. Berhanu and M. H. Ranje, 1989: A Finite Element Computer Program for Dynamic Simulate of Thermal and Fluid Systems, Proc. 1989 ASEE Annual Conference, 2, 788-791.

A Finite Element Computer Program for Dynamic Simulation of Thermal and Fluid Systems

Joseph Chi
Eskinder Berhanu
Mohammad H. Ranje
Mechanical Engineering
University of The District of Columbia
Washington, DC

ABSTRACT

Computer-aided modeling of thermal and fluid systems has gained acceptance both in scientific research and industrial design. Typical CAD/CAE systems for thermal/fluid modeling include a finite element analysis code and graphic facilities for pre- and post-processing. The authors have developed at UDC several thermal/fluid systems simulation computer programs [1-3]. A finite element analysis computer program UDCFLOW has now been integrated with the PATRAN graphic software package for finite element pre- and post-processing. In order to introduce students to the new material and to demonstrate to students that the engineer must stay abreast of current developments, UDCFLOW and PATRAN software packages are being used to teach students at UDC the transient characteristics of fluid flow and heat transfer.

INTRODUCTION

Traditional introductory fluid mechanics and heat transfer courses cover simple fluid flow and heat transfer problems in a sequential and compartmental fashion. Studies of the transient fluid flow and heat transfer problems are often limited to those problems for which either the closed-form solutions or tabulated functions are readily available. By providing students with a finite element fluid/thermal analysis computer program integrated with the graphic pre- and post-processor, the depth and breadth, as well as the students' mastery of materials covered in the fluid/thermal courses, can be increased over the traditional approach.

Generalized computer programs which allow a wide variety of fluid/thermal systems to be modeled and simulated have recently been developed and they are becoming commercially available. Examples of these programs include Fidap, Flotran, Fluent and Phoenics [4,5]. However, source codes for these programs are not available to students, and no single software is always superior to the others. For classroom adaptation, it is necessary to have a program developed by the instructor for the instructional purpose of relieving the students of arithmatical drudgery, permitting them the routine solution of more involved problems, and developing their ability to modify programs for dealing with new phenomena. For this objective, the authors have developed a UDCFLOW finite element fluid/thermal analysis computer program.

In this paper, the UDCFLOW computer program is described first. Interface of UDCFLOW with PATRAN finite element graphic pre- and post-processing software package is then reviewed. Finally, examples of coursework that uses the UDCFLOW/PATRAN softwares are presented.

UDCFLOW FINITE ELEMENT COMPUTER PROGRAM AND PATUDC FOR PATRAN/UDCFLOW INTERFACING

UDCFLOW is a general-purpose computer program which is being developed at the University of the District of Columbia. To facilitate efficient simulation under a wide variety of conditions, the UDCFLOW has been intergrated with the PATRAN software package for graphic pre- and post-processing of the finite element analysis. Although the UDCFLOW computer program is being developed for simulating 3-D heat, mass and momentum transfer. For use in the undergraduate classroom, a version of UDCFLOW for solving the general 1-D heat, mass and momentum transfer problems has been employed.

The governing equation for the general 1-D convection and diffusion problem can be written as:

$$A\frac{\partial T}{\partial t} + AU\frac{\partial T}{\partial x} = \frac{Ah}{\rho C_p}(T_e - T) + \frac{qA}{\rho C_p} + \frac{\partial}{\partial x}\left(\frac{kA}{\rho C_p}\frac{\partial T}{\partial x}\right) \quad (1)$$

and the required boundary conditions for the problem are as follows:

$$\text{At } x=0: \quad -[(kA/\rho C_p)\partial T/\partial x]_o = \gamma_o T_{e,o} + \sigma_o \quad (2)$$

$$\text{At } x=L: \quad [(kA/\rho C_p)\partial T/\partial x]_\ell = \gamma_\ell T_{e,\ell} + \sigma_\ell \quad (3)$$

In the above equations, t is the time, x the coordinate, T the temperature, U the velocity, A the cross-sectional area, Λ the perimeter, ρ the density, C_p the specific heat, k the thermal conductivity, h the heat transfer coefficient, q the heat source per unit volume and T_e the environmental temperature, and γ_o, σ_o, γ_ℓ and σ_ℓ are constant values at the domain boundary.

Professor and Chairman
Teaching Assistants

The Galerkin finite element spatial discretization of equations (1) to (3) leads to a system of coupled nonlinear ordinary differential equations:

$$[C]\{a\}' + [K]\{a\} + \{S\} = 0 \qquad (4)$$

Here, [C] is the capacitance matrix, [K] the sum of convective and conductance matrix, {S} the source vector, and {a} the time-dependent temperature values at nodal points of the solution domain. A Newton-Raiphson iterative procedure [6] has been used to solve the equation set (4) for the {a(t,x)} values, and a computer program UDCFLOW has been developed to facilitate the calculations. In addition, UDC has developed an interface between the PDA's PATRAN modeling software and the UDC's UDCFLOW finite element analysis computer program.

The PATRAN program provides an interactive, graphics-oriented environment for creation of a geometric and finite-element model and for display of analysis results. The interface allows PATRAN to be used for the model creation and post-processing steps and UDCFLOW to be used for the analysis. The interface consists of a stand-alone translator program PATUDC that will read the PATRAN model data and transform it into a UDCFLOW input file. After fluid/thermal analysis by UDCFLOW is complete, the results can be transferred back to PATRAN for post-processing display.

CLASSROOM ADAPTATION AND WORKED EXAMPLES

For classroom instruction of the thermal/fluid system modeling using the PATRAN and UDCFLOW softwares, students may first be introduced to the use of PATRAN to generate geometric and finite element models for a variety of fluid/thermal systems. They will then learn to run the UDC developed PATRAN/UDCFLOW interface computer program PATUDC which will read PATRAN model data and transform them into UDCFLOW input files. Source codes for a version of the UDCFLOW computer program will then be given to the students. After the students have familiarized themselves with the UDCFLOW program, they will be assigned to solve a number of problems with different degrees of complexity. Several examples of these problems are presented below.

To illustrate the procedure, we will begin with a simple 1-D transient heat conduction problem, with known boundary temperatures. This will be followed by more difficult transient problems which begin to display the power and importance of the modeling, analysis and display softwares.

Consider an infinite slab of thickness 0.3 meter which was discussed in reference [7]. Initially because of an electrical current passing the slab, the slab is in the steady state with a temperature distribution in degrees C is given by the equation:

$$T = 100 + 400\sin(\pi x/0.3). \qquad (5)$$

However, at time t=0, the electric current is shut off, thus causing a transient in the temperature, while the slab faces continue to be held at 100 degrees C by a coolant. The thermal diffusisity of the material is constant at the value of $2.84\times10^{-5}m^2/s$. We would like to find the temperature within the slab as a function of position and time by using the PATRAN/UDCFLOW softwares.

A model for this problem can easily be created by using the following PATRAN commands:

```
GR,1,,0
GR,2,TR,0.3,1
LI,1,ST,,1,2
GF,1L,G,33
CF,1L,BAR
PM,1,TAN,...
PM,2,TAN,...
PM,3,TAN,...
PM,4,TAN,...
PM,5,TAN,...
PM,6,TAN,...
DF,1L,...,1
```

The PATRAN output file PATRAN.OUT can then be read by PATUDC interface program to produce a UDCFLOW.DAT file which can be read by the UDCFLOW finite element analysis program. Output file from the UDCFLOW run, UDCFLOW.RST, can then be used by the PATRAN post-processor P/PLOT to produce the X-Y plot of temperature versus time. Figure 1 shows temperature distributions of the slab at time equal to 0, 150, 300, 450, and 750 seconds, respectively.

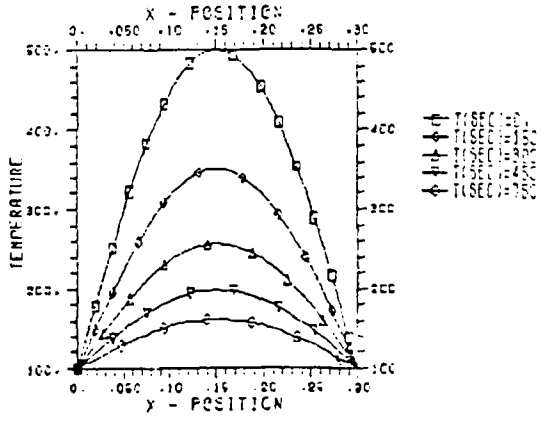

Fig. 1 Simulated Transient Slab Temperature

For problems with exitance of combined convective, diffusion and internal energy source, let us consider, for example, a problem which has the following data:

$$\begin{aligned} A &= 0.0013952 \text{ ft} \\ q &= 2{,}400 \sin(x/L) \\ \rho &= 50 \text{ lb/ft} \\ U &= 1.2 \text{ ft/s} \\ C_p &= 1.1 \text{ Btu/lb.F} \\ k &= 1.028 \text{ But/ft.F.s.} \end{aligned} \qquad (6)$$

Initially, the fluid is uniformly at 200 degrees F. At t greater than zero, the temperature of the fluid is held at 200 degrees at x equal to zero, and gradient of the temperature dT/dx is maintained to be zero at x equal to L. Figure 2 shows resultant temperature distributions of the fluid at several different time periods of t equal to 1, 2, 3, 5, and 9 seconds, respectively.

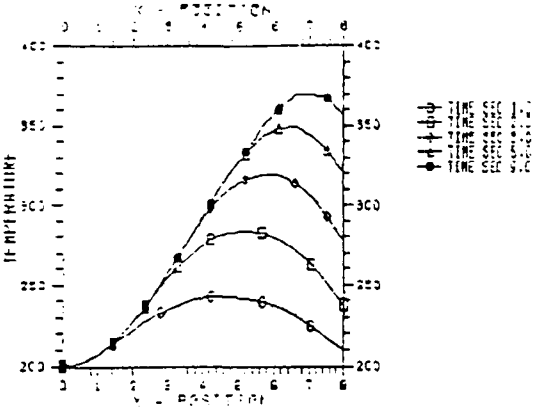

Fig. 2 Simulated Transient Fluid Temperature

CONCLUSIONS

Computer-aided modeling of thermal and fluid systems has gained acceptance both in scientific research and industrial design. Typical CAD/CAE systems for fluid/thermal modeling include finite element analysis code and graphic facilities for pre- and post-processing. To instruct the students early in their career, the authors have developed at UDC a finite element fluid/thermal analysis computer program UDCFLOW which has been integrated with the PDA's interactive graphics-oriented finite element modeling pre- and post-processing software PATRAN. It resulted in an efficient system which the students can use to gain hands-on experience in computer-aided modeling of the fluid/thermal systems and to solve more involved problems than was previously possible. It is hoped that this will enhance the students' learning experience and increase their problem solving abilities.

ACKNOWLEDGEMENT

This work has been partially supported by the Office of Naval Research; the authors wish to express their appreciation for its support.

REFERENCES

[1] Chi, J., (1977): "Numerical Analysis of Turblent End-Wall Boundary Layers of Intense Vortices," J. Fluid Mech., Vol.82/Pt.2, pp.309-333.

[2] Chi, J., (1987): "Heat, Moisture and Momentum Transfer in Turbulent Vortex Flows Over the Water Surface," Proc. 1987 ASME/JSME Thermal Engineering Conference, pp.627-633.

[3] Chi, J., (1988): "CADSES--A Computer-Aided Design System for Simulation Studies of Energy Systems," Proc. 1988 ASEE Annual Conference, pp.777-781.

[4] Iannuzzelli, R, and Hutchings, B, (1986): "Fluid Dynamics Software Gets Down to Work," Mechanical Engineering, Vol.109/No.7, pp.60-63.

[5] Hutchings, B., and Iannuzzelli, R, (1987): "Fluid Dynamics Software: A First Look," Mechanical Engineering, Vol.110/No.5, pp.72-76.

[6] Baker, A.J and M.O. Soliman, (1982): "Current Topics on Finite Element Analysis for Flows with Large Reynolds Number," Proc. International Symposium on Finite Element Flow Analysis, pp.129-136.

[7] Sucec, J., (1985): "Heat Transfer," Wm. C. Brown Publishers, Dubuque, Iowa, 837pp.

JOSEPH CHI, PH.D., P.E.

Professor Joseph Chi received his B.S. and Ph.D. Degrees from the University of London, London, England, in 1960 and 1965, respectively, and he is a registered professional mechanical engineer in the District of Columbia. He has since 1966 held faculty positions at the Catholic University of America, the George Washington University, and the University of the District of Columbia, and he has also been employed by the National Bureau of Standards for two years. He holds presently a position of Chairman and Professor in the Department of Mechanical Engineering at the University of the District of Columbia, and the Chairman of the ASME Washington D.C. Section. He has published two textbooks and over 50 research papers in the areas of engineering education, heat transfer, fluid mechanics, and computer applications.

ESKINDER BERHANU, M.S.

Eskinder Berhanu received his B.S. in Mechanical Engineering from Addis Ababa University in 1983 and his M.S. in Mechanical Engineering from Howard University in 1988. He is currently working as a research engineer at the at Mechanical Engineering department of the University of the District of Columbia.

MOHAMMAD H. RANJE, M.S.

Mohammad H. Ranje received his B.S. in Mechanical Engineering from University of the District of Columbia in 1982 and his M.S. in Mechanical Engineering from Howard University in 1988. He is currently working toward a Ph.D. Degree at Howard University.